UNIVERSITY OF KWA-ZULU NATAL

SIGNAL SPACE COOPERATIVE COMMUNICATION WITH PARTIAL RELAY SELECTION

Zaid Paruk

Supervised By: Professor Hongjun Xu

2012

SIGNAL SPACE COOPERATIVE COMMUNICATION WITH PARTIAL RELAY SELECTION

Zaid Paruk

Supervised By: Professor Hongjun Xu

Submitted in fulfilment of the degree of Master of Engineering,
School of Engineering, University of Kwa-Zulu Natal, Durban, South Africa

February 2012

As the candidate’s supervisor I agree to the submission of this dissertation.

Date of Submission: _____

Supervisor: _____

Professor Hongjun Xu

Declaration

I, Zaid Paruk, declare that,

i. The research reported in this dissertation, except where otherwise indicated, is my original work.

ii. This dissertation has not been submitted for any degree or examination at any other university.

iii. This dissertation does not contain other persons' data, pictures, graphs or other information, unless specifically acknowledged as being sourced from other persons.

iv. This dissertation does not contain other persons' writing, unless specifically acknowledged as being sourced from other researchers. Where other written sources have been quoted, then:

   a. Their words have been re-written but the general information attributed to them has been referenced;

   b. Where their exact words have been used, their writing has been placed inside quotation marks, and referenced.

v. Where I have reproduced a publication of which I am an author, co-author or editor, I have indicated in detail which part of the publication was actually written by myself alone and have fully referenced such publications.

vi. This dissertation does not contain text, graphics or tables copied and pasted from the Internet, unless specifically acknowledged, and the source being detailed in the dissertation and in the References sections.

Signed: _____

Acknowledgements

I would firstly like to thank my supervisor, Professor Hongjun Xu, for the motivation and guidance I received throughout the writing of this work. His passionate approach to research and his dedication both to his students and to his field is truly an inspiration. I would secondly like to thank Telkom for their support in this endeavour.

Thirdly, my thanks go to my family who put up with the many hours spent researching and writing. Without their support this would never have been possible. Finally, I would like to express my gratitude to my loving wife for her continued support and encouragement during the production of this work, and for her assistance with the production of the included diagrams.

Abstract

Exploiting the available diversity from various sources in wireless networks is an easy way to improve performance at the expense of additional hardware, space, complexity and/or bandwidth. Signal space diversity (SSD) and cooperative communication are two promising techniques that exploit the available signal space and space diversity respectively. This study first presents symbol error rate (SER) analysis of an SSD system containing a single transmit antenna and N receive antennas with maximal-ratio combining (MRC) reception; thereafter it presents a simplified maximum-likelihood (ML) detection scheme for SSD systems, and finally presents the incorporation of SSD into a distributed switch and stay combining with partial relay selection (DSSC-PRS) system.

Performance analysis of an SSD system containing a single transmit antenna and multiple receive antennas with MRC reception has been presented previously in the literature using the nearest neighbour (NN) approximation to the union bound, however results were not presented in closed form. Hence, closed form expressions are presented in this work. A new lower bound for the SER of an SSD system is also presented which is simpler to evaluate than the union bound/NN approximation and also simpler to use with other systems. The new lower bound is based on the minimum Euclidean distance of a rotated constellation and is termed the minimum distance lower bound (MDLB); it is also presented here in closed form. The presented bounds have been validated with simulation and found to be tight under certain conditions.

The SSD scheme offers error performance and diversity benefits with the only penalty being an increase in detector complexity. Detection is performed in the ML sense and conventionally, all points in an M-ary quadrature amplitude modulation (M-QAM) constellation are searched to find the transmitted symbol. Hence, a simplified detection scheme is proposed that only searches m symbols from M after performing initial signal conditioning. The simplified detection scheme is able to provide SER performance close to that of optimal ML detection in systems with multiple receive antennas.

Cooperative communication systems can benefit from the error performance and diversity gains of the spectrally efficient SSD scheme since it requires no additional hardware, bandwidth or transmit power. Integrating SSD into a DSSC-PRS system has shown an improvement of approximately 5dB at an SER of 10^{-4} with a slight decrease in spectral efficiency at low SNR. Analysis has been performed using the newly derived MDLB and confirmed with simulation.

Table of Contents

List of Figures

List of Tables

List of Acronyms

4D CR	4-Dimensional Constellation Rotation
AF	Amplify-and-Forward
AWGN	Additive White Gaussian Noise
C-MRC	Cooperative Maximal-Ratio Combining
CSI	Channel State Information
DF	Decode-and-Forward
DSC	Distributed Selection Combining
DSSC	Distributed Switch and Stay Combining
i.i.d	Independent and Identically Distributed
MDLB	Minimum Distance Lower Bound
ML	Maximum-Likelihood
MRC	Maximal-Ratio Combining
PAM	Pulse Amplitude Modulation
PDF	Probability Density Function
PEP	Pairwise Error Probability
PRS	Partial Relay Selection
QAM	Quadrature Amplitude Modulation
SC	Selection Combining
SDF	Selective Decode-and-Forward
SER	Symbol Error Rate
SLB	Sphere Lower Bound
SNR	Signal-to-Noise Ratio

SSC	Switch and Stay Combining
SSD	Signal Space Diversity
TDMA	Time Division Multiple Access
WLAN	Wireless Local Area Network

Part I

Introduction

1. Introduction

Wireless communication has seen accelerated growth in recent years. It is increasingly becoming not just a means of transmitting voice but also a means of accessing services such as broadband internet, teleconferencing, and streaming video. These services are being delivered over a wide variety of wireless networks including wireless local area networks (WLAN), city wide or even inter-city networks, and the increasing predominant and ubiquitous cellular networks. Wireless networking technologies, while being updated constantly, have been unable to keep up with the increasing demands for higher data rates, greater coverage and increased user capacity.

The mobile communication paradigm places a unique blend of constraints on the wireless communication system. Processing power, transmit power and physical space are all limited at mobile nodes. Moreover, by their mobile nature, mobile terminals often face severe signal degradation due to the effects of large and small scale fading [1]. Spatial diversity is a common technique used to combat the effects of fading and is steadily becoming a primary method of increasing performance in mobile wireless networks.

Cooperative communication has been proposed [2, 3] as a spatial diversity technique to combat the effects of fading in mobile terminals that often do not have the space required to implement multiple transmit/receive antennas (although the newly released Apple iPhone 4S does make use of transmit and receive diversity [4]). By making use of additional relay nodes in the communication process, network coverage can be expanded and natural resilience to shadowing and fading can be attained. Cooperative communication, however, also has the fundamental problem of reduced spectral efficiency due to the re-transmission of signals by relaying nodes. This reduction in spectral efficiency worsens with an increase in the number of participating relays, however, it can be somewhat mitigated by careful system design.

Making optimal use of the available diversity from the addition of cooperating nodes often means using complex combiners at the receiver [5–7]. Lowering the complexity at the receiver, necessary for mobile terminals, also results in significant error performance and diversity losses. This motivates research into methods of improving error performance and spectral efficiency in low complexity cooperative communication systems. Signal space diversity (SSD) is proposed as a diversity method that does not require additional space or bandwidth to improve error performance and provide diversity gains, and hence is ideal for mobile wireless networks [8].

The issue of complexity is significant when dealing with mobile cellular networks. Hence, in this work, significant attention is paid to decreasing the complexity of the network wherever possible, while maximising the available diversity.

1.1 Cooperative Communication

Cooperative communication makes use of additional 'relay' (R) nodes in the communication process to relay information between the conventional source (S) and destination (D) nodes. The relays provide additional independent paths for signal propagation between the source and destination and hence provide the possibility of spatial diversity. The independent paths created from the relays and source to the destination can be imagined to form a 'virtual' antenna array at the destination [9], similar to the independent paths created by a physical antenna array with sufficient spacing. A typical relay network can be visualized in Figure 1.1.

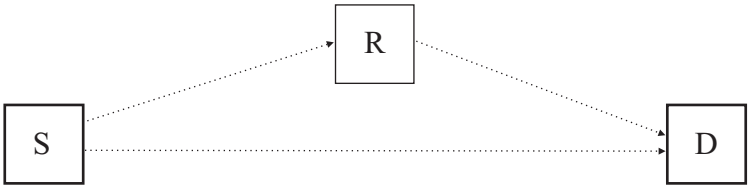

Figure 1.1: Typical cooperative communication system with a single relay

Employing cooperative communication necessitates the re-transmission of information from the relay(s) on orthogonal channels, usually subsequent time slot(s). Doing so presents the obvious problem of decreased spectral efficiency, especially as the number of relays, N, gets larger. This can be somewhat mitigated by system design, usually at the expense of error performance [10]. Regardless, cooperative communication yields obvious benefits with regards to the mitigation of fading and increased coverage of a network. Opportune placement of relays can also assist signal propagation around large natural objects which would otherwise hamper such propagation.

1.1.1 Relaying Strategies

A 'relaying strategy' broadly refers to the way received signals are processed by the relay before re-transmission. Various levels of performance can be attained depending on the level of complexity at the relay and at the destination.

The simplest relaying strategy from a processing point of view is amplify-and-forward (AF). With AF, the relay simply amplifies the received analogue waveform with an amplification factor G and then re-transmits without any other processing. Enforcing a typical average transmit power constraint at the relay, the amplification factor is bounded by [9]:

$$G \leq \sqrt{\frac{E_S}{|h_{SR}|^2 E_S + N_0}} \tag{1.1}$$

where E_S is the average energy per symbol, $|h_{SR}|^2$ is the fading power between the source and the relay node, and N_0 is the noise power spectral density. When the AF strategy is used in an N relay cooperative system, full diversity of $N+1$ can be achieved at the destination node with the use of maximal-ratio combining (MRC) [11]. However, the AF strategy requires the storage of analogue waveforms at the relay before re-transmission which can be prohibitive.

Decode-and-forward (DF) is a regenerative strategy that first decodes the received information and thereafter re-encodes and re-transmits it. This mitigates the need to store analogue waveforms at the relay and is thus simple to implement. However, DF suffers from potential error propagation due to possible decoding errors at the relay, thus making the source-relay-destination ($S - R - D$) channel non-linear and non-Gaussian [6]. The DF strategy can therefore not guarantee full diversity without additional processing at either the relay or destination. Further, the end-to-end equivalent signal-to-noise ratio (SNR) of the dual-hop $S-R-D$ link is not known due to the mentioned properties. However, in [6, Property 1], the dual-hop equivalent SNR was found to be upper bounded by the minimum of the two single hop SNRs. In the analysis, it was shown that the error rate achieved using the bound was tight in the high SNR region.

Various selective decode-and-forward (SDF) relaying schemes have also been proposed in the literature which use SNR thresholds, CRC codes, or similar error detection techniques to detect possible decoding errors at the relay [12, 13]. Received symbols are then not forwarded if the SNR threshold is not met or if errors are detected when decoding. Such schemes are able to achieve full diversity since error propagation is mitigated; however when coding is used to determine forwarding, spectral efficiency is further reduced.

1.1.2 Cooperative Communication Schemes

Uncoded cooperative communication schemes are reviewed here with emphasis on their complexity and achievable diversity order.

As mentioned, the DF relaying strategy cannot collect full diversity at the receiver without additional processing. In [2, 3], a λ-MRC detector at the destination was presented which weights the signals received by the destination from the relay with a factor λ before employing MRC to combine all received signals. It was shown that full diversity could then be collected at the destination. However, the parameter λ was not found analytically and was used as an upper bound on the maximum error performance attainable.

In [6], it was shown that while the optimal maximum-likelihood (ML) detector can collect full diversity at the destination, ML detection becomes prohibitively complex with larger than binary constellations. A cooperative-MRC (C-MRC) combiner was proposed at the destination which weights the signals arriving from the relay node at the destination according to:

$$w_{RD} = \frac{\gamma_{eq}}{\gamma_{RD}} h_{RD}^{*} \tag{1.2}$$

where w_{RD} is the weight being designed, γ_{eq} and γ_{RD} are the equivalent $S-R-D$ channel and $R-D$ channel instantaneous SNRs respectively, h_{RD} is the fading coefficient of the $R-D$ link, and $(\cdot)^{*}$ denotes the complex conjugate. This C-MRC scheme, similar to the λ-MRC proposed in [2, 3], achieves full diversity when used at the destination along with an accompanying reduction in complexity relative to ML detection.

Smart relaying [5, 7], scales transmit power at the relay to compensate for a weak $S-R$ channel relative to the $R-D$ channel, achieving full diversity at the cost of requiring feedback from the destination at the relay. It was further shown that by using soft power scaling at the relay, i.e. scaling using the average $R-D$ channel SNR, no feedback is required to achieve full diversity in exchange for slightly decreased error performance. Smart relaying and C-MRC were both easily extended to multi-hop and multi-relay cooperative networks independent of modulation [5–7].

The diversity-multiplexing problem, tackled in [10], shows that optimal diversity-multiplexing trade-off can be achieved. However, in the interests of attaining maximum spectral efficiency, relay selection has been proposed which selects a single 'best' relay from N total based on some criterion, usually the two-hop channel characteristics [14–17]. This also circumvents the need for complex time and carrier synchronization between relay nodes. Communication thus takes place in two time slots only and thus improves spectral efficiency compared to N relay forwarding schemes while still enabling the use of multiple relays to give full diversity. However, a combiner is still required at the destination to combine signals from the source and the best relay.

Employing switch and stay combining (SSC) at the destination as in [18] to give a distributed switch and stay combining (DSSC) 'antenna' array between the source and relay nodes mitigates the need for a combiner at the destination. This was extended to a dual-relay system that does not make use of the direct $S - D$ link in [19]. In [20], a DSSC system was proposed for multiple relays, making use of relay selection to choose a single relay to participate as the relayed branch of the DSSC system. However, this requires feedback from the destination to select the best relay as the selection is made based on two-hop channel characteristics.

A partial relay selection (PRS) scheme was proposed in [11] using the AF relaying strategy. PRS uses only the first hop ($S - R$) SNR when choosing the best relay from N. This mitigates the need for feedback from the destination to the relay nodes. In [11], diversity from cooperation was not achieved due to the lack of a direct $S - D$ link. DSSC with PRS was proposed in [21] for the DF relaying strategy, enabling multiple relays to be used in a DSSC system without feedback from the destination for relay selection. Employing SSC at the destination also improves spectral efficiency since there is no need for two time slots when the direct link is active. It was shown in [21] that additional diversity order is attained with the use of a direct $S - D$ link, however an increase in the number of relays participating in the PRS protocol does not improve error performance above $N = 3$ relays nor diversity order above a single relay.

It is clear that from a complexity and spectral efficiency standpoint, the DSSC-PRS system provides advantages over other systems. However, the achieved error performance is far lower than that achievable by schemes such as C-MRC and does not scale with the addition of relays to the system. This motivates the addition of the SSD technique which improves error performance and diversity order with no bandwidth, transmit power or space penalty. Thus, the relatively high spectral efficiency of the system is maintained.

1.2 Signal Space Diversity

Multi-dimensional constellations can provide 'signal space' diversity by exploiting the inherent diversity present in the different dimensions of the constellation. By subjecting the individual dimensions to independent fading, it was found that diversity order up to the minimum number of distinct points in a constellation is possible [22], with the only disadvantage being an ML detector with increased complexity at the receiver, and no bandwidth, space or transmit power penalty. A simple rotation operation on a typical two-dimensional M-QAM constellation increases the minimum number of distinct components

present between any two points in the constellation; this is illustrated on a typical 4-QAM constellation in Figure 1.2. Interleaving the in-phase and quadrature components of a symbol pair before transmission and de-interleaving after transmission results in no fading correlation between the in-phase and quadrature components of a symbol.

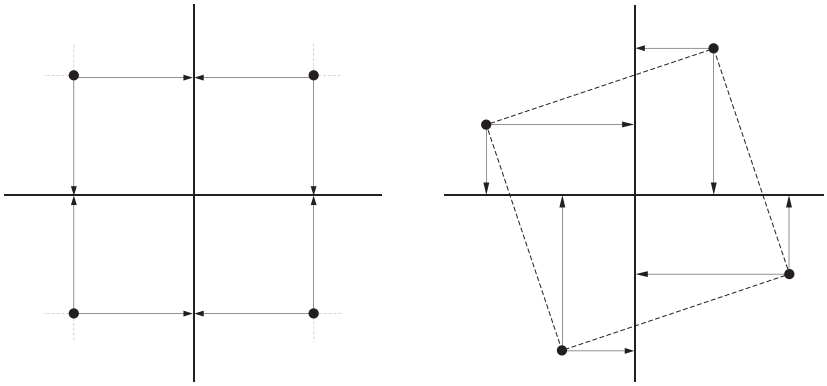

Figure 1.2: Increasing the minimum number of distinct components for 4-QAM

Early work on multi-dimensional constellations focused on carving effective constellations from lattices in n-dimensional space and matching them to fading channels [23]. The idea of rotating a constellation and interleaving the components to provide diversity gains was first presented in [24]. Thereafter, the problem of carving a constellation from the rotated cubic lattice Z^n to achieve the highest diversity order was tackled in [22]. It was found that multi-dimensional constellations, generated by the Cartesian product of $n/2$ two-dimensional constellations, could be found with diversity order high enough to approach Gaussian channel error performance with the only drawback being increased detector complexity.

SSD is thus an extremely spectral and power efficient method of increasing performance in a system with minimal increase in complexity, making it an ideal candidate to improve performance in a system with low complexity as a design criterion. Digital terrestrial video broadcasting system DVB-T2 already makes use of rotated constellations for performance improvements [25].

Rotating a two-dimensional constellation results in every point being uniquely identifiable from either of its components, a fact well exploited in the signal space cooperation scheme proposed in [26]. In that system, the relay is able to generate the second symbol in an interleaved symbol pair by merely detecting the first symbol correctly. This results in the system obtaining a diversity order of two and the mentioned benefits of cooperative communication, but not the maximum possible benefit of diversity from SSD and from cooperative communication.

Constellation rotation in SSD schemes has traditionally been performed via real rotation matrices. However, complex rotation matrices are possible [27–29] and provide error performance gains relative to real rotation matrices with an increase in overall system complexity. SSD has also been applied to cooperative communication systems. In [30], SSD was used in a coded DF cooperative system resulting in additional diversity order benefits, however no analysis was given. In [31], SSD was added to a DF cooperative system with knowledge of correct reception at the relay and M-PSK modulation. Analysis showed that a diversity order increase from SSD was achieved and that optimal power allocation at the relay could provide further error performance improvements.

Diversity order and error performance can be improved by performing an additional rotation and interleaving stage [32]. The additional rotation and interleaving stage brings a further diversity order of two at the expense of increased ML detector complexity relative to a single stage. Termed 4-dimensional constellation rotation (4D CR), the 4D SSD system was found to outperform conventional 2D SSD systems; however no analytical results were presented.

In most studies, error probability of SSD systems is evaluated with the union bound [22, 26, 33–35] or the nearest neighbour (NN) approximation; presented for M-PSK in [33] and M-QAM with receive MRC in [36], however the expressions in [36] were not presented in closed form. Error performance of uncoded rotated lattice constellations has also been evaluated with the sphere lower bound (SLB) [37], performed by integration over the Voronoi region presented in [38]. Exact expressions for the error rates of SSD systems were presented in [39, 40] for both Rayleigh and Rician fading channels. However, these were not presented in closed form and require numerical evaluation of complicated integrals. Thus, an expression for the error probability of SSD systems that is simple to compute and is easily applied to other systems does not yet exist.

Conventional ML detection for SSD requires an exhaustive search among all points in the constellation to find the point closest in Euclidean distance to the received signal [22]. Therefore, the possibility of developing detection schemes which simplify processing requirements at the receiver exists and will be explored in this work.

2. Motivation and Research Objective

Error performance evaluation of a system with M-QAM SSD modulation, a single transmit antenna and N receive antennas with MRC reception was presented using the NN approximation to the union bound in [36], however, analytical expressions were not presented in closed form. This motivates the derivation of closed form expressions based on the union bound and NN approximation for a similar system.

Error performance evaluated using the union bound requires computation of the Euclidean distance between all constellation points in a rotation constellation [22, 34], and exact results in [39, 40] require numerical evaluation of integrals. This motivates the derivation of a new lower bound on the SER of an SSD system based on the minimum Euclidean distance of a rotated constellation which is simple to compute and easily applied to other systems. The new lower bound will also be presented in closed form for the system mentioned above.

Conventional ML detection for SSD systems requires an exhaustive search among all points in a rotated constellation to find the transmitted symbol [22]. This motivates the development of a simplified ML detection scheme that only searches m points from M, where M denotes the cardinality of the constellation. The achieved SER of the simplified detection scheme will be compared with that of optimal ML detection using simulation.

The DSSC-PRS system provides diversity benefit from cooperation and attains better spectral efficiency than conventional cooperative systems [21]; however, error performance can still be improved. This motivates the application of SSD to DSSC-PRS to provide diversity and error performance improvements without bandwidth, transmit power or space penalty.

3. Contributions of Included Papers

The contributions of the dissertation are presented in two papers prepared for submission to peer reviewed journals, summarized below. The papers are presented in Part II of this dissertation and concluding remarks are presented in Part III.

3.1 Paper A

Z. Paruk and H. Xu, "Performance Analysis and Simplified Detection for Signal Space Diversity with MRC Reception," 2012.

In Paper A, closed form SER expressions are presented for a system employing M-QAM SSD modulation, a single transmit antenna and N receive antennas with MRC reception using the union bound and the NN approximation in Rayleigh fading. A new lower bound on the SER based on the minimum Euclidean distance of a rotated constellation is also presented in closed form. Analytical results for the derived bounds are validated with simulations in Rayleigh fading channels with differing values of N. A simplified detection scheme for ML detection of SSD symbols is also presented, with simulation results shown for systems containing single and multiple receive antennas.

3.2 Paper B

Z. Paruk and H. Xu, "Distributed Switch and Stay Combining with Partial Relay Selection and Signal Space Diversity," 2012.

In Paper B, the SSD scheme is incorporated into a DSSC-PRS network. Analytical results are derived in the form of a lower bound on the SER, making use of the lower bound derived in Paper A and further approximations to find the SER of the system. Results are validated with simulation and the spectral efficiency of the new system is derived and compared with the non-SSD system implementation as well as other cooperative systems.

4. Future Work

The derived SER lower bound for SSD, while fairly tight across the SNR range, is not exact. Hence, the need for a simple, exact, closed form expression for the error performance of SSD systems still exists and the problem of finding such an expression is still an open one. Further, the simplified detection scheme presented does not achieve optimal error performance or full diversity in single transmit/receive antenna systems. Therefore, the possibility of simplified detection schemes that achieve optimal performance is another topic for future investigation.

Distributed switched/selective systems are attractive for their spectral efficiency and simplicity. However, there still exists further scope for research into distributed switched/selective systems with improved error performance, diversity and spectral efficiency. A variety of techniques could be used to improve error performance such as the decision statistic for selection systems proposed in [41]. This work could also be extended to the case of relays of different types as well as relays which contain information of their own to transmit to the destination. The effects of feedback imperfections when selecting the best relay in the DSSC-PRS-SSD system could also be studied.

5. References

[1] A. Goldsmith, *Wireless Communications*. Cambridge: Cambridge Univ. Press, 2005.

[2] A. Sendonaris, E. Erkip, and B. Aazhang, "User cooperation diversity - Part I: System description," *IEEE Trans. Commun.*, vol. 51, no. 11, pp. 1927–1938, Nov. 2003.

[3] —, "User cooperation diversity - Part II: Implementation aspects and performance analysis," *IEEE Trans. Commun.*, vol. 51, no. 11, pp. 1939–1948, Nov. 2003.

[4] *Certification test report for iPhone with GSM WCDMA 1xRTT/CDMA 1xEVDO rev.a, Bluetooth EDR 2.1, Bluetooth 4.0 LE, and WiFi 802.11 bgn*, Fremont, CA, U.S.A: Compliance Certification Services (UL CSS), Oct. 2011. [Online]. Available: https://apps.fcc.gov/eas/GetApplicationAttachment.html?id=1553679.

[5] N. H. Vien, H. H. Nguyen, and T. Le-Ngoc, "Diversity analysis of smart relaying," *IEEE Trans. Veh. Technol.*, vol. 58, no. 6, pp. 2849–2862, Jul. 2009.

[6] T. Wang, A. Cano, G. B. Giannakis, and J. N. Laneman, "High-performance cooperative demodulation with decode-and-forward relays," *IEEE Trans. Commun.*, vol. 55, no. 7, pp. 1427–1438, Jul. 2007.

[7] T. Wang, G. B. Giannakis, and R. Wang, "Smart regenerative relays for link-adaptive cooperative communications," *IEEE Trans. Commun.*, vol. 56, no. 11, pp. 1950–1960, Nov. 2008.

[8] N. H. Tran, H. H. Nguyen, and T. Le-Ngoc, "BICM-ID with signal space diversity over cascaded Rayleigh fading channels," *IEEE Trans. Commun.*, vol. 56, no. 10, pp. 1561–1568, Oct. 2008.

[9] J. N. Laneman, D. N. C. Tse, and G. W. Wornell, "Cooperative diversity in wireless networks: Efficient protocols and outage behavior," *IEEE Trans. Inf. Theory*, vol. 50, no. 12, pp. 3062–3080, Dec. 2004.

[10] K. Azarian, H. El Gamal, and P. Schniter, "On the achievable diversity-multiplexing tradeoff in half-duplex cooperative channels," *IEEE Trans. Inf. Theory*, vol. 51, no. 12, pp. 4152–4172, Dec. 2005.

[11] I. Krikidis, J. Thompson, S. McLaughlin, and N. Goertz, "Amplify-and-forward with partial relay selection," *IEEE Commun. Lett.*, vol. 12, no. 4, pp. 235–237, Apr. 2008.

[12] M. Janani, A. Hedayat, T. E. Hunter, and A. Nosratinia, "Coded cooperation in wireless communications: Space-time transmission and iterative decoding," *IEEE Trans. Signal Process.*, vol. 52, no. 2, pp. 362–371, Feb. 2004.

[13] J. Hu and N. C. Beaulieui, “Performance analysis of decode-and-forward relaying with selection combining,” *IEEE Commun. Lett.*, vol. 11, no. 6, pp. 489–491, Jun. 2007.

[14] Z. Yi and I. Kim, “Diversity order analysis of the decode-and-forward cooperative networks with relay selection,” *IEEE Trans. Wireless Commun.*, vol. 7, no. 5, pp. 1792–1799, May 2008.

[15] M. Abouelseoud and A. Nosratinia, “Opportunistic relay selection with a direct link,” in *Proc. Global Telecommunications Conf.*, 2010, pp. 1–5.

[16] Y. Jing and H. Jafarkhani, “Single and multiple relay selection schemes and their achievable diversity orders,” *IEEE Trans. Wireless Commun.*, vol. 8, no. 3, pp. 1414–1423, Mar. 2009.

[17] Y. Zhao, R. Adve, and T. J. Lim, “Symbol error rate of selection amplify-and-forward relay systems,” *IEEE Commun. Lett.*, vol. 10, no. 11, pp. 757–759, Nov. 2006.

[18] D. S. Michalopoulos and G. K. Karagiannidis, “Distributed switch and stay combining (DSSC) with a single decode and forward relay,” *IEEE Commun. Lett.*, vol. 11, no. 5, pp. 408–410, May 2007.

[19] —, “Two-relay distributed switch and stay combining,” *IEEE Trans. Commun.*, vol. 56, no. 11, pp. 1790–1794, Nov. 2008.

[20] V. N. Q. Bao and H. Y. Kong, “Distributed switch and stay combining for selection relay networks,” *IEEE Commun. Lett.*, vol. 13, no. 12, pp. 914–916, Dec. 2009.

[21] —, “Distributed switch and stay combining with partial relay selection over Rayleigh fading channels,” *IEICE Trans. Commun.*, vol. 93, no. 10, pp. 2795–2799, Oct. 2010.

[22] J. Boutros and E. Viterbo, “Signal space diversity: A power- and bandwidth-efficient diversity technique for the Rayleigh fading channel,” *IEEE Trans. Inf. Theory*, vol. 44, no. 4, pp. 1453–1467, Jul. 1998.

[23] J. Boutros, E. Viterbo, C. Rastello, and J.-C. Belfiore, “Good lattice constellations for both Rayleigh fading and Gaussian channels,” *IEEE Trans. Inf. Theory*, vol. 42, no. 2, pp. 502–518, Mar. 1996.

[24] K. Boulle and J.-C. Belfiore, “Modulation scheme designed for the Rayleigh fading channel,” presented at the CISS’92, Princeton, NJ, Mar. 1992.

[25] *Frame structure channel coding and modulation for a second generation digital terrestrial television broadcasting system (DVB-T2)*, European Standard, ETSI EN 302 755, Sep. 2009.

[26] S. A. Ahmadzadeh, S. A. Motahari, and A. K. Khandani, “Signal space cooperative communication,” *IEEE Trans. Wireless Commun.*, vol. 9, no. 4, pp. 1266–1271, Apr. 2010.

[27] A. Correia, “Optimised complex constellations for transmitter diversity,” *Wireless Pers. Commun.*, vol. 20, no. 3, pp. 267–284, 2002.

[28] A. Correia and A. Hottinen, “Complex constellations for WCDMA with transmitter diversity,” in *Proc. IEEE 6th Int. Symp. on Spread Spectrum Techniques and Applications*, vol. 2, 2000, pp. 439–443.

[29] A. Correia, A. Hottinen, and R. Wichman, “Optimised constellations for transmitter diversity,” in *Proc. IEEE 50th Vehicular Technology Conf.*, vol. 3, 1999, pp. 1785–1789.

[30] W. Ning, Z. Zhongpei, and L. Shaoqian, “Signal space diversity in decode-and-forward cooperative communication,” in *Proc. WRI Int. Conf. Communications and Mobile Computing*, 2009, pp. 127–130.

[31] N. F. Kiyani, U. H. Rizvi, and G. Dolmans, “Modulation diversity benefits in cooperative communications,” in *Proc. Wireless Telecommunications Symp.*, 2010, pp. 1–5.

[32] J. Kim, H. Kim, T. Jung, J. Bae, and G. Lee, “New constellation-rotation diversity scheme for DVB-NGH,” in *IEEE 72nd Vehicular Technology Conf.*, 2010, pp. 1–4.

[33] N. F. Kiyani, J. H. Weber, A. G. Zajic, and G. L. Stuber, “Performance analysis of a system using coordinate interleaving and constellation rotation in Rayleigh fading channels,” in *Proc. IEEE 68th Vehicular Technology Conf.*, 2008, pp. 1–5.

[34] G. Taricco and E. Viterbo, “Performance of component interleaved signal sets for fading channels,” *IEE Electronics Letters*, vol. 32, no. 13, pp. 1170–1172, Apr. 1996.

[35] N. H. Tran, H. H. Nguyen, and T. Le-Ngoc, “Performance of BICM-ID with signal space diversity,” *IEEE Trans. Wireless Commun.*, vol. 6, no. 5, pp. 1732–1742, May 2007.

[36] S. Jeon, I. Kyung, and M.-S. Kim, “Component-interleaved receive MRC with rotated constellation for signal space diversity,” in *IEEE 70th Vehicular Technology Conf. Fall*, 2009, pp. 1–6.

[37] A. G. I. Fabregas and E. Viterbo, “Sphere lower bound for rotated lattice constellations in fading channels,” *IEEE Trans. Wireless Commun.*, vol. 7, no. 3, pp. 825–830, Mar. 2008.

[38] J.-C. Belfiore and E. Viterbo, “Approximating the error probability for the independent Rayleigh fading channel,” in *Proc. Int. Symp. Information Theory*, 2005, pp. 362–362.

[39] J. Kim and I. Lee, “Analysis of symbol error rates for signal space diversity in Rayleigh fading channels,” in *Proc. IEEE Int. Conf. on Communications*, 2008, pp. 4621–4625.

[40] J. Kim, W. Lee, J.-K. Kim, and I. Lee, “On the symbol error rates for signal space diversity schemes over a Rician fading channel,” *IEEE Trans. Commun.*, vol. 57, no. 8, pp. 2204–2209, Aug. 2009.

[41] Y. G. Kim and S. W. Kim, “Optimum selection diversity for BPSK signals in Rayleigh fading channels,” *IEEE Trans. Commun.*, vol. 49, no. 10, pp. 1715–1718, Oct. 2001.

Part II

Included Papers

Paper A

Performance Analysis and Simplified Detection for Signal Space Diversity with MRC Reception

Z. Paruk and H. Xu

Prepared for submission to SAIEE Africa Research Journal.

Abstract

Signal space diversity (SSD) is a promising technique for obtaining diversity without increases in bandwidth, transmit power or physical hardware at the expense of increased ML detection complexity. Symbol error rate (SER) analysis of a system containing a single transmit antenna and N receive antennas with maximal-ratio combining (MRC) reception is presented here along with a simplified detection scheme for SSD systems. The union bound and the nearest neighbour (NN) approximation are presented in closed form, and a new, simpler SER bound for SSD systems based on the minimum Euclidean distance of a rotated constellation is presented, also in closed form. Performance of the new bound is found to be tight for low signal-to-noise ratios (SNRs), small rotation angles and when the number of receive antennas (N) is large; the new bound is also easily applied to other systems. The simplified detection scheme, while losing diversity and SER performance when $N = 1$, achieves a 7dB and 4dB performance improvement over non-SSD transmission at SERs of 10^{-3} and 10^{-2} for 4-QAM and 16-QAM respectively. However, when $N \geq 3$, SER performance is close to indistinguishable from that of optimal ML detection while achieving complexity reductions of up to 25%, 75% and 93% for 4-QAM, 16-QAM and 64-QAM respectively.

1. Introduction

Diversity schemes typically rely on multiple copies of a transmitted signal arriving at the receiver over independent channels, which may be orthogonal in time or frequency or separated in space. These redundant copies available at the destination may then be combined in various ways [1] depending on the processing and hardware constraints at the receiver. Typically, spatial diversity schemes use multiple transmit and/or receive antennas [2] to generate the redundant signal copies. Spatial diversity, while capable of providing substantial gains, requires additional antennas and enough distance between them to avoid correlation at either the transmitter or receiver and hence is not a practical solution in all cases.

A diversity technique which has not seen much attention is signal space diversity (SSD) [3]. SSD exploits the inherent diversity available in the different dimensions of a multi-dimensional constellation by ensuring that different components are each affected by independent fading. Consequently, no additional bandwidth, transmit power or space is required, however this is achieved at the cost of necessitating a more complicated maximum-likelihood (ML) detector at the receiver. This makes SSD a useful technique in the modern mobile communication focused age, as more processing power becomes available in mobile devices but space constraints are not lifted. Second generation digital terrestrial television systems already employ rotated constellations to provide error performance and diversity gains [4].

It was demonstrated in [5] that the union bound could be used to evaluate error performance of rotated constellations with component interleaving by summing over the pairwise error probabilities (PEP) between any arbitrary constellation point and every other constellation point. The pairwise error probability has been found in closed form in [5] and [6] for M-QAM and PSK modulations respectively, and is sometimes used in conjunction with the Chernoff bound [5]. The union bound, while asymptotically tight, is loose at low signal-to-noise (SNR) and for larger constellations [7], while the Chernoff bound is looser by close to 4dB [5].

The nearest neighbour (NN) approximation approximates the union bound by only considering the PEP of the nearest neighbours of any constellation point. The NN approximation was presented in [8] for MRC reception and M-QAM modulation, and in [6] for PSK modulation. However, no closed form solution was presented for M-QAM with MRC reception in [8].

Recently, exact error expressions have been derived for SSD systems by introducing a change in signal model and by using polar coordinates for both Rayleigh [9] and Rician [10] channels. The new signal model takes the ratio of the standard deviation of the in-phase

and quadrature components into account, and hence states that the resulting decision regions become non-perpendicular. The conditional probability of error is then integrated over these non-perpendicular regions defined by the angles between them using polar coordinates. The derived expressions, while accurate, are not presented in closed form and require numerical evaluation of integrals.

Also recently, a lower bound for uncoded rotated lattice constellations based on the sphere lower bound (SLB) was proposed in [11] for Nakagami-m fading. The SLB shown in [11] is based on the integration of the Voronoi region shown in [7]. It was shown that the SLB exhibits good performance for infinite lattices regardless of the lattice structure. However for finite multi-dimensional constellations obtained from the rotation of M-PAM (Pulse Amplitude Modulation) constellations, the SLB only exhibits tight performance as M gets large.

An accurate and simple to compute closed form expression for the error probability of rotated multi-dimensional constellations with SSD that is also easy to use with other systems does not yet exist. In this study, we attempt to derive such an expression in the form of a lower bound based on the minimum Euclidean distance of a rotated constellation. The lower bound is presented in closed form and compared with the union bound and NN approximations, which are also presented here in closed form, for a system containing a single transmit antenna and multiple receive antennas with MRC reception.

The optimal ML detection rule requires an exhaustive search among all constellation points before estimating the transmitted symbol. Hence, the possibility of reducing the complexity of ML detection exists. A simplified detection scheme is presented here which searches constellation points from a total of M after performing initial signal conditioning. The performance of the simplified detection scheme is compared to that of the optimal detection scheme using simulation for both single and multiple antenna reception.

The rest of this paper is organized as follows: Section 2 presents the system model, Section 3 presents performance analysis of the various bounds, Section 4 presents the simplified detection scheme, results are presented in Section 5 and Section 6 presents concluding remarks.

2. System Model

A multi-dimensional constellation is said to be capable of L order diversity when the minimum number of unique components between any two points of the constellation is L. Consider the conventional (S) and rotated ($\tilde{S}$) constellations shown in Figure A.1. Clearly, rotating the constellation maximizes the minimum number of distinct components between any two points in the constellation while retaining the same average energy, given by the expectation $E[S^2]$, where $E[\cdot]$ denotes the expectation operator. Thus, in the absence of fading (AWGN channel), the rotated set $\tilde{S}$ exhibits the same performance as the conventional set S.

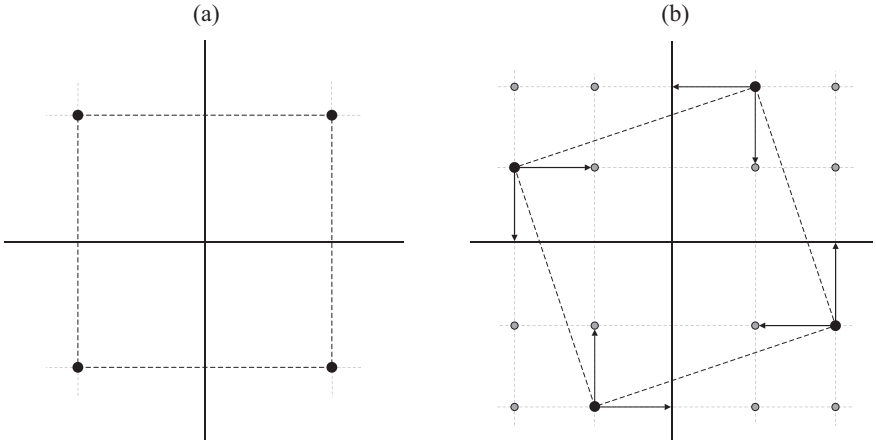

Figure A.1: (a) original constellation S and (b) rotated constellation $\tilde{S}$ showing expansion

We formally define S to be a signal set such that $S = \left\{ s_l^I + j s_l^Q : l = 0, 1, ..., M-1 \right\}$, where M denotes the cardinality of S, and $(\cdot)^I$, $(\cdot)^Q$ refer to the in-phase and quadrature part of a signal respectively. The rotated set $\tilde{S}$ is then obtained by applying a rotation matrix $\mathbf{R}^\theta$ to each element of S according to $\tilde{s}_l = \mathbf{R}^\theta s_l$, for a rotation of angle θ. For a two-dimensional constellation, the rotation matrix takes the form [12]:

$$\mathbf{R}^\theta = \begin{bmatrix} cos\theta & -sin\theta \\ sin\theta & cos\theta \end{bmatrix} \tag{A.1}$$

To obtain diversity, the unique components need to be affected by independent fading. This is achieved by a component interleaver/de-interleaver present at the transmitter and receiver respectively. Performing the interleaving/de-interleaving action ensures that a single deep fade will not affect all components of the signal simultaneously, thus achieving signal space diversity. Note that the rotated constellation, once component interleaved, now forms an expanded constellation equivalent to the Cartesian product of the in-phase and quadrature

components of the original constellation set, defined as $\tilde{S}_E = S^I \times S^Q$, where $\times$ denotes the Cartesian product. This can be visualized in Figure A.1.

We now consider the system with block diagram shown in Figure A.2. Consider a network containing a source node with a single transmit antenna and a destination node containing N receiving antennas, also referred to here as N independent branches. The receive antennas are spaced far enough apart for there to be no correlation among the respective received signals. There is no feedback channel between the destination and source nodes and no source or channel coding is performed.

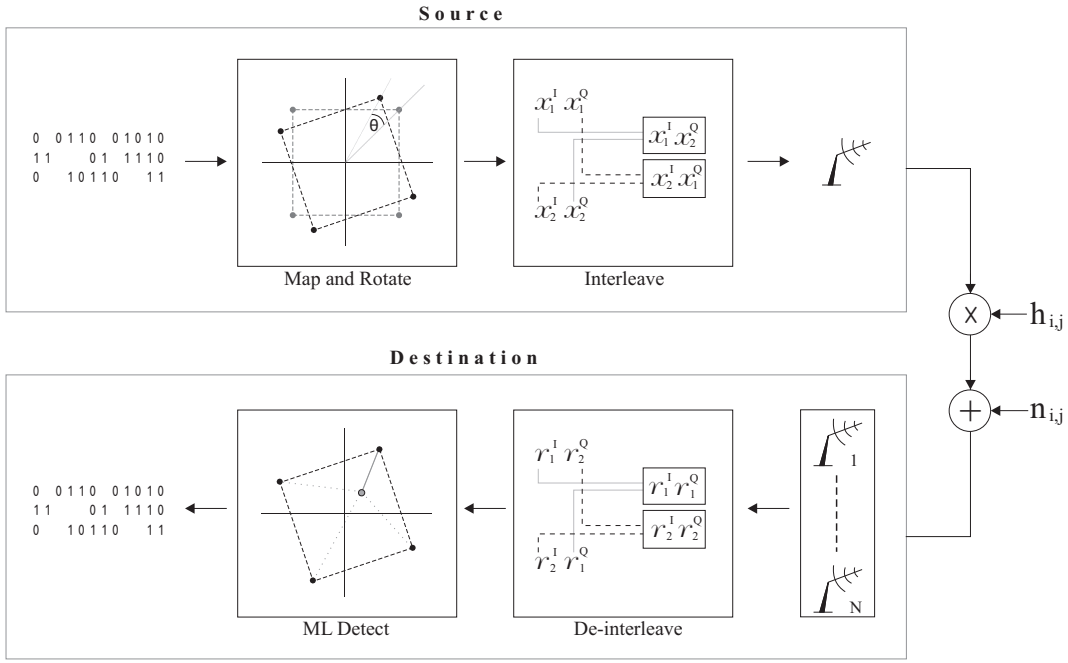

Figure A.2: Block diagram of SSD system with MRC reception

Following the system block diagram, a bit stream is mapped to symbols denoted $x = x^I + jx^Q$ from the rotated constellation $\tilde{S}$ as shown in the first block in Figure A.2, which are then arbitrarily grouped into pairs of symbols and passed through a component interleaver, shown in the second block. The component interleaver interleaves the in-phase and quadrature components of the symbols in each pair to give new symbols u_t, $t \in \{1, 2\}$, where t is the index of a symbol in a symbol pair. A typical interleaved symbol pair is shown below:

$$\begin{aligned} u_1 &= x_1^I + jx_2^Q \\ u_2 &= x_2^I + jx_1^Q \end{aligned} \tag{A.2}$$

The interleaved symbols u_t are then transmitted by the single transmit antenna and arrive at the destination over N i.i.d (independent and identically distributed) Rayleigh fading channels with additive white Gaussian noise from the N receive antennas. Each symbol u_t in a symbol pair is transmitted over an orthogonal channel, assumed to be independent time slots in this study. Transmission occurs in two subsequent time slots, with u_1 transmitted in the first time slot and u_2 in the second. Therefore, the SSD system consumes no more bandwidth than comparable non-SSD systems. Thus we denote the received symbols to be $r_{i,j}$, where the subscript $i \in \{1, 2\}$ is the orthogonal channel (time slot) index and the subscript $j \in \{1, 2, ..., N\}$ is the receive antenna index. The received symbols at antenna j are then given by:

$$r_{i,j} = h_{i,j}u_t + n_{i,j} \tag{A.3}$$

where $h_{i,j}$ is the fading coefficient in time slot i at antenna j. We assume that full channel state information (CSI) of all paths is available at the receiver and that no inter-symbol interference occurs, hence the receiver is able to remove the phase shift induced by fading. Thus the fading is modelled as independent Rayleigh distributed random variables with amplitude distributed according to $f_h\left(h_{i,j}\right) = \frac{h_{i,j}}{\sigma^2}\exp\left(\frac{-h_{i,j}^2}{2\sigma^2}\right)$ and unit second moment, i.e. $E\left[h_{i,j}^2\right] = 2\sigma^2 = 1$. The fading is assumed to be flat. The transmitted signals are perturbed by additive white Gaussian noise, modelled as circular symmetric Gaussian random variables with distribution $n_i \sim \mathcal{CN}\left(0, N_0\right)$, i.e. zero mean and variance $N_0/2$ per dimension.

Diversity combining is performed at the destination in the optimal fashion using MRC. Symbols are combined on a symbol-by-symbol basis as they are received, however detection is only performed after a symbol pair from all N antennas has been received, combined and de-interleaved. Combining is performed by weighting the received signal from each path with the respective instantaneous fading coefficient for that path. This gives the combined signal for time slot i:

$$r_i = h_{i,1}r_{i,1} + h_{i,2}r_{i,2} + ... + h_{i,N}r_{i,N} \tag{A.4}$$

where we have defined the combined signal to be r_i. This is similar to combining in a non-SSD system, and combines the branches in the optimal fashion. We further define an instantaneous combined fading term based on the sum of the individual instantaneous branch fading powers:

$$h_i^2 = h_{i,1}^2 + h_{i,2}^2 + ... + h_{i,N}^2 \tag{A.5}$$

De-interleaving is then performed on a symbol pair to ensure that the in-phase and quadrature components of the original symbol are reassembled before detection. The symbols are then detected in the ML sense after de-interleaving, assuming full CSI. For MRC reception, the ML rule can be written as, for both time slots [13, 14]:

$$\begin{aligned}\hat{x}_1 &= \arg\min_{x_k \in \tilde{S}} \left\{ h_2^2 \left| r_1^I - h_1^2 x_k^I \right|^2 + h_1^2 \left| r_1^Q - h_2^2 x_k^Q \right|^2 \right\} \\ \hat{x}_2 &= \arg\min_{x_k \in \tilde{S}} \left\{ h_1^2 \left| r_2^I - h_2^2 x_k^I \right|^2 + h_2^2 \left| r_2^Q - h_1^2 x_k^Q \right|^2 \right\}\end{aligned} \tag{A.6}$$

where h_i^2 has been defined in (A.5), and $\hat{x}_i$ are the detected symbols for time slot i. Note the addition of the combined fading coefficient in each term of the ML decision rule, e.g. the h_2^2 in $h_2^2 \left| r_1^I - h_1^2 x_k^I \right|^2$.

3. Performance Analysis

In this section we first review the conventional approach to approximating the error probability of SSD systems based on the union bound as presented in [3, 5, 6]. We then review the NN approximation [8] and present it in closed form, since the NN approximation often has tighter error performance, especially at low SNR. We thereafter present a simpler minimum Euclidean distance based lower bound which is applicable to any square M-QAM constellation.

For convenient discussion, we use $f(x)$ to denote the PDF of random variable x, $F(x)$ to denote its CDF, and $P(z)$ to denote the probability of event z.

3.1 Union Bound

The union bound gives a standard method of evaluating the error probability of an arbitrary signal set by summing the PEPs across all possible transmit and receive pairs. The union bound P_S^U on the symbol error probability (SER) is given as [5]:

$$P_S^U(e) \leq \frac{1}{\left|\tilde{S}\right|} \sum_{x \in \tilde{S}} \sum_{\substack{\hat{x} \in \tilde{S} \\ x \neq \hat{x}}} P(x \to \hat{x}) \tag{A.7}$$

where $\left|\tilde{S}\right|$ denotes the cardinality of the signal set and $P(x \to \hat{x})$ is the unconditional PEP of the detector choosing $\hat{x}$ given that x was transmitted. Letting $y_i = h_i^2(E_S/N_0)$ be the combined instantaneous SNR in time slot i, the conditional PEP follows from the ML rule expressed in equation (A.6) and can be written as [5]:

$$\begin{aligned} P(x \to \hat{x}|h_1, h_2) &= P\left(\|\mathbf{r} - \mathbf{h}\odot\mathbf{x}\|^2 \geq \|\mathbf{r} - \mathbf{h}\odot\hat{\mathbf{x}}\|^2 |h_1, h_2\right) \\ &= P\left(\|\mathbf{n}\|^2 \geq \|\mathbf{r} - \mathbf{h}\odot\hat{\mathbf{x}}\|^2 |h_1, h_2\right) \\ &= Q\left(\sqrt{\frac{1}{2N_0}\left(h_1^2 d_1^2 + h_2^2 d_2^2\right)}\right) \\ &= Q\left(\sqrt{\frac{1}{2E_S}\left(\gamma_1^2 d_1^2 + \gamma_2^2 d_2^2\right)}\right) \end{aligned} \tag{A.8}$$

where $\mathbf{r} = \left(r^I, r^Q\right)$, $\mathbf{h} = (h_1, h_2)$, $\mathbf{x} = \left(x^I, x^Q\right)$ and $\hat{\mathbf{x}} = \left(\hat{x}^I, \hat{x}^Q\right)$ are the two-dimensional received signal, channel coefficient, transmitted and chosen signal vectors respectively, the $\|\cdot\|$ operation represents the vector norm, the $\odot$ operation represents the vector product, E_S is the average energy per symbol, and d_1^2, d_2^2 represent the in-phase and quadrature distances between

x and $\hat{x}$ respectively. Averaging the conditional PEP over the independent fading distributions for MRC reception gives the unconditional PEP:

$$P\left(x \to \hat{x}\right) = \int_0^\infty \int_0^\infty Q\left(\sqrt{\frac{1}{2E_S}\left(\gamma_1^2 d_1^2 + \gamma_2^2 d_2^2\right)}\right) f_{\gamma_{MRC}}\left(\gamma_1\right) f_{\gamma_{MRC}}\left(\gamma_2\right) d\gamma_1 d\gamma_2 \quad \text{(A.9)}$$

Closed form expressions for the PEP have been shown in [5] and [6] for M-QAM and PSK modulations respectively in Rayleigh fading with a single transmit/receive antenna. Substituting (A.9) into (A.7) yields the final union bound on the error probability.

The NN approximation can be used to simplify the union bound by considering only the points closest in Euclidean distance to any symbol in a constellation [6, 8]. For small constellations such as 4-QAM the NN approximation is equivalent to the union bound [6]. The NN approximation was presented in [8] for a system employing MRC reception, however no closed form expressions were presented. We thus present closed form expressions for the NN approximation with N-branch receive MRC using the trapezoidal approximation to the $Q\left(\cdot\right)$ function, presented later in this section.

Following the approach presented in [8], the NN approximation for 4-QAM is equivalent to the union bound since the nearest points constitute the entire constellation. For 16-QAM, the NN approximation can be written, by considering the points in the corners, centre, and sides of the constellation, as [8]:

$$P_{16-QAM}^{NN}\left(e\right) = \frac{1}{4}P_{corner}\left(e\right) + \frac{1}{4}P_{centre}\left(e\right) + \frac{1}{2}P_{side}\left(e\right) \quad \text{(A.10)}$$

where $P_{corner}\left(e\right)$, $P_{centre}\left(e\right)$, and $P_{side}\left(e\right)$ are the error probabilities of the points located at the corners, centre and sides of the constellation respectively. Each of the described points has perpendicular and diagonal neighbours with different Euclidean distances. By considering the different neighbours, the NN approximation for 16-QAM can be written as[1] :

$$\begin{aligned} P_{16-QAM}^{NN}\left(e\right) = &\frac{1}{4}\left[2P_{perp}\left(x \to \hat{x}\right) + P_{diag}\left(x \to \hat{x}\right)\right] + \\ &\frac{1}{4}\left[4P_{perp}\left(x \to \hat{x}\right) + 4P_{diag}\left(x \to \hat{x}\right)\right] + \\ &\frac{1}{2}\left[3P_{perp}\left(x \to \hat{x}\right) + 2P_{diag}\left(x \to \hat{x}\right)\right] \\ = &\,3P_{perp}\left(x \to \hat{x}\right) + \frac{9}{4}P_{diag}\left(x \to \hat{x}\right) \end{aligned} \quad \text{(A.11)}$$

[1]Equation (21) in [13] incorrectly calculates the number of diagonal neighbours for $P_{centre}\left(e\right)$ and $P_{side}\left(e\right)$, the corrected calculation is presented here.

where $P_{perp}\left(x \rightarrow \hat{x}\right)$ and $P_{diag}\left(x \rightarrow \hat{x}\right)$ are the PEPs between any point and its perpendicular and diagonal neighbours respectively. The PEPs can be found directly by substituting the relevant distances into (A.9). These distances are easily computed for perpendicular and diagonal neighbours as[1] :

$$\begin{array}{ll} d^2_{1_{perp}} = 4\cos^2\theta & d^2_{2_{perp}} = 4\sin^2\theta \\ d^2_{1_{diag}} = 4\left(1+\sin 2\theta\right) & d^2_{2_{diag}} = 4\left(1-\sin 2\theta\right) \end{array} \tag{A.12}$$

After making the relevant substitutions, integrating over the fading distributions gives the final PEP. We make use of the trapezoidal approximation to the $Q\left(x\right)$ function shown in [15] to simplify analysis. The $Q\left(\cdot\right)$ function can be approximated as:

$$Q\left(\delta\right) = \frac{1}{2n}\left(\frac{1}{2}\exp\left(\frac{-\delta^2}{2}\right) + \sum_{c=1}^{n-1}\exp\left(\frac{-\delta^2}{S_c}\right)\right) \tag{A.13}$$

where $S_c = 2\sin^2\left(c\pi/2n\right)$ and n is the total number of iterations used in the approximation. The PEP can thereafter be written using (A.9), (A.12) and (A.13) for N-branch MRC reception as:

$$\begin{aligned} P\left(x \rightarrow \hat{x}\right) = & \int_0^\infty \int_0^\infty \left[\frac{1}{2n}\left(\frac{1}{2}\exp\left(\frac{-\chi}{2}\right) + \sum_{i=1}^{n-1}\exp\left(\frac{-\chi}{S_i}\right)\right)\right] \times \\ & f_{\gamma_{MRC}}\left(\gamma_1\right) f_{\gamma_{MRC}}\left(\gamma_2\right) d\gamma_1 d\gamma_2 \\ = & \frac{1}{4n}\left(\frac{2}{\rho^2_{1_z}\overline{\gamma}+2}\right)^N \left(\frac{2}{\rho^2_{2_z}\overline{\gamma}+2}\right)^N + \\ & \frac{1}{2n}\sum_{i=1}^{n-1}\left(\frac{S_i}{\rho^2_{1_z}\overline{\gamma}+S_i}\right)^N \left(\frac{S_i}{\rho^2_{2_z}\overline{\gamma}+S_i}\right)^N \end{aligned} \tag{A.14}$$

where $\chi = \frac{1}{2E_S}\left(\gamma_1^2 d_1^2 + \gamma_2^2 d_2^2\right)$, $f_{\gamma_{MRC}}\left(\gamma_i\right) = \frac{1}{(N-1)!}\frac{1}{\overline{\gamma}^N}\gamma_i^{N-1}\exp\left(\frac{-\gamma_i}{\overline{\gamma}}\right)$ is the well-known MRC PDF for N receive antennas, $\rho^2_{i_z} = \left(d^2_{i_z}/2E_S\right)$ and z refers to the $diag$ or $perp$ distances in (A.12). Substituting the relevant distances from (A.12) into (A.14) and thereafter (A.14) into (A.11) gives the final NN approximation to the union bound for N-branch MRC reception for 16-QAM. The expression in (A.14) can also be used in the union bound shown in (A.7) after computing and substituting the relevant distances.

[1]The diagonal distance is reported incorrectly in [13]. The corrected distance is shown here.

3.2 Minimum Distance Lower Bound

The union bound sums the PEPs between any transmitted symbol and all possible received symbols to upper bound the SER, making use of the squared Euclidean distance between the points under consideration. We now derive a lower bound on the SER using the minimum Euclidean distance of the constellation, taking into consideration the independent fading on the individual components of the signal set.

The minimum Euclidean distance of a binary constellation is sometimes used to quantify its performance [16]. We now extend the concept to larger constellations. The minimum Euclidean distance (hereafter referred to as the minimum distance) is defined as:

$$d_{min} = \min_{x_k, x_l \in S} \left\{ \sqrt{|x_k - x_l|^2} \right\} \tag{A.15}$$

where x_k, x_l are any symbols from a signal set S. For a conventional square M-QAM constellation, the minimum distance can easily be shown to be $d_{min} = \sqrt{2d}$, where d is the relative size of the constellation.

The minimum distance of a constellation is not affected by rotation. However, in a system employing SSD, the individual components of the signal are affected by independent fading due to the interleaving and de-interleaving action. We therefore modify the minimum distance calculation to account for the fading on the individual components of the signal:

$$d_{min} = \min_{x_k, x_l \in \tilde{S}} \left\{ \sqrt{h_1^2 \left| x_k^I - x_l^I \right|^2 + h_2^2 \left| x_k^Q - x_l^Q \right|^2} \right\} \tag{A.16}$$

where h_1 and h_2 refer to the independent fading affecting the in-phase and quadrature parts of the signal from the first and second time slot respectively. This in effect is the minimum distance of the constellation after the rotation, interleaving, transmission over fading channel, and de-interleaving operations. Now, due to the independent fading on the individual dimensions, the minimum distance is dependent on the rotation angle.

For square M-QAM constellations, the minimum distance is easily calculated from any constellation point to any of its closest constellation points along a rotated perpendicular axis. Figure A.3 illustrates this graphically.

Assuming that an M-QAM constellation has a spacing of two in each dimension between neighbouring constellation points, the minimum distance for a rotated two-dimensional constellation $\tilde{S}$ can be computed as:

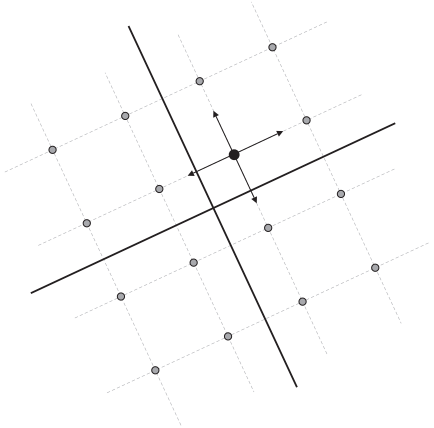

Figure A.3: Closest points for minimum distance calculation

$$d_{min}^{\tilde{S}} = \sqrt{4h_1^2 \cos^2\theta + 4h_2^2 \sin^2\theta} \tag{A.17}$$

The conventional square M-QAM SER conditioned upon the instantaneous SNR can be written as [17]:

$$P_S^{M-QAM}(e|\gamma) = 4aQ\left(\sqrt{b\gamma}\right) - 4a^2Q^2\left(\sqrt{b\gamma}\right) \tag{A.18}$$

where $a = \left(1 - \frac{1}{\sqrt{M}}\right)$ and $b = \frac{3}{M-1}$. We again make use of the trapezoidal approximation to the $Q(x)$ and $Q^2(x)$ functions shown in [15] to simplify analysis. The conditional M-QAM SER for any square M-QAM constellation can be written using the mentioned approximations as:

$$\begin{aligned} P_S^{M-QAM}(e|\gamma) &= 4aQ\left(\sqrt{b\gamma}\right) - 4a^2Q^2\left(\sqrt{b\gamma}\right) \\ &= \frac{a}{n}\left\{\begin{array}{l} \frac{1}{2}\exp\left(\frac{-b\gamma}{2}\right) - \frac{a}{2}\exp\left(-b\gamma\right) + \\ (1-a)\sum_{c=1}^{n-1}\exp\left(\frac{-b\gamma}{S_c}\right) + \sum_{c=n}^{2n-1}\exp\left(\frac{-b\gamma}{S_c}\right) \end{array}\right\} \end{aligned} \tag{A.19}$$

where $S_c = 2\sin^2 c\pi/4n$. The factor $\sqrt{d_{min}^2/2N_0}$ can be substituted into the conditional SER in (A.19) (similar to the factor $\sqrt{d_i^2/2N_0}$ in the PEP in (A.8)) in place of $\sqrt{b\gamma}$ to give (A.20). Doing so lower bounds the SER since not all error events are taken into consideration. We henceforth term the new lower bound the minimum distance lower bound (MDLB).

$$P_S^{MDLB}\left(e|h_1,h_2\right) \geq 4aQ\left(\sqrt{\frac{d_{min}^2}{2N_0}}\right) - 4a^2Q^2\left(\sqrt{\frac{d_{min}^2}{2N_0}}\right) \tag{A.20}$$

After some simple manipulations, we arrive at the final conditional MDLB on the SER in equation (A.21), with the terms a and b defined as they were in (A.18), and defining $\gamma_i = h_i^2\left(E_S/N_0\right)$ to be the combined instantaneous SNR from the N receive antennas. Notice now that the final conditional MDLB resembles the exact conditional M-QAM SER with the instantaneous SNR changed to represent the independent fading on each dimension and the SSD rotation angle:

$$P_S^{MDLB}\left(e|\gamma_1,\gamma_2\right) \geq 4aQ\left(\sqrt{b\zeta}\right) - 4a^2Q^2\left(\sqrt{b\zeta}\right) \tag{A.21}$$

where $\zeta = \left(\gamma_1\cos^2\theta + \gamma_2\sin^2\theta\right)$. The conditional MDLB is then averaged over both fading distributions to give the final bound on the error probability:

$$\begin{aligned} P_S^{MDLB}\left(e\right) \geq \int_0^\infty\int_0^\infty \left\{4aQ\left(\sqrt{b\zeta}\right) - 4a^2Q^2\left(\sqrt{b\zeta}\right)\right\} \times \\ f_{\gamma_{MRC}}\left(\gamma_1\right) f_{\gamma_{MRC}}\left(\gamma_2\right) d\gamma_1 d\gamma_2 \end{aligned} \tag{A.22}$$

Substituting the relevant fading distributions for MRC with N receive antennas and then performing the double integration gives the final expression for the unconditional MDLB:

$$P_S^{MDLB}\left(e\right) \geq \frac{a}{n}\left\{\begin{array}{l} \frac{1}{2}\left(\frac{2}{\alpha b\overline{\gamma}+2}\right)^N\left(\frac{2}{\beta b\overline{\gamma}+2}\right)^N - \\ \frac{a}{2}\left(\frac{1}{\alpha b\overline{\gamma}+1}\right)^N\left(\frac{1}{\beta b\overline{\gamma}+1}\right)^N + \\ (1-a)\sum_{c=1}^{n-1}\left(\frac{S_c}{\alpha b\overline{\gamma}+S_c}\right)^N\left(\frac{S_c}{\beta b\overline{\gamma}+S_c}\right)^N + \\ \sum_{c=n}^{2n-1}\left(\frac{S_c}{\alpha b\overline{\gamma}+S_c}\right)^N\left(\frac{S_c}{\beta b\overline{\gamma}+S_c}\right)^N \end{array}\right\} \tag{A.23}$$

where $\alpha = \cos^2\theta$, $\beta = \sin^2\theta$ and $\overline{\gamma} = E\left[\gamma\right]$. The new MDLB can be easily computed, is free from any complicated mathematical functions due to the approximations used, is presented in closed form, and can easily be applied to any system already using the conditional square M-QAM SER expression from (A.18) by making a simple substitution.

4. Simplified Detection

The conventional ML detection rule in (A.6) performs an exhaustive search among all points in a constellation to find the one closest in squared Euclidean distance to the received symbol using the ML decision criterion. While providing optimal error performance, this is far from efficient. We thus propose a sub-optimal simplified detection scheme that first equalises the received symbols and then, after de-interleaving, selects the point closest in Euclidean distance to the equalized symbol. A search using the ML decision criterion is then performed among the m points closest to the equalised point, where $1 \leq m \leq M$. The new ML detection rule thus significantly reduces the complexity of ML detection in terms of the number of searches required.

The simplified detection scheme is split into two phases: the equalisation and selection phase, and the search phase. As with conventional ML detection, symbols can only be detected once both symbols in a symbol pair have been received and de-interleaved. The equalisation and selection phase first equalises the symbols received in each time slot by dividing by the known fading coefficient for that time slot to give symbols y_i. A typical equalised symbol pair is shown below, where the equalization is performed knowing that h_i (defined in (A.5)) is an amplitude distribution:

$$\begin{aligned} y_1 &= \frac{r_1}{h_1} = u_1 + \frac{n_1}{h_1} \\ y_2 &= \frac{r_2}{h_2} = u_2 + \frac{n_2}{h_2} \end{aligned} \tag{A.24}$$

Equalising the received symbols now gives the original transmitted symbols u_i together with noise from each time slot scaled by the fading coefficient. Note that the symbols u_i are still component interleaved; they must now be de-interleaved to reassemble the respective in-phase and quadrature components together.

The selection part of the first phase uses a simple boundary check to choose a symbol from the original constellation S closest to the equalised symbol y_i. However, since the equalised symbols are rotated, they must first be un-rotated before the boundary check is performed. The un-rotation operation is performed by applying the rotation matrix from (A.1) with an angle of $-\theta$. Thereafter, the boundary check is performed on both in-phase and quadrature components of the equalised symbol to determine the location of the closest symbol from S, denoted v, $v \in S$.

The search phase uses the location of symbol v to create a new symbol set $\tilde{T}$ (which is a subset of $\tilde{S}$) consisting of $m-1$ symbols closest to v and v itself. The symbol set $\tilde{T}$ for each symbol v can be pre-determined and stored, and hence need not be recreated for every received symbol. This can be visualized in Figure A.4, where $m = 5$ and the diamond represents the location of symbol v after rotation. A conventional ML search is then performed on the new symbol set $\tilde{T}$, as opposed to the entire rotated set $\tilde{S}$. This greatly reduces the complexity of ML detection required for SSD systems employing large constellations.

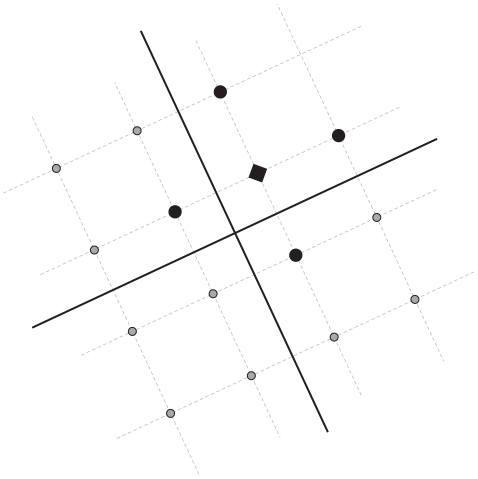

Figure A.4: Location of $m = 5$ closest points

The new ML rule can thus be expressed as:

$$\begin{aligned} \hat{x}_1 &= \arg\min_{x_k \in \tilde{T}} \left\{ h_2^2 \left| r_1^I - h_1^2 x_k^I \right|^2 + h_1^2 \left| r_1^Q - h_2^2 x_k^Q \right|^2 \right\} \\ \hat{x}_2 &= \arg\min_{x_k \in \tilde{T}} \left\{ h_1^2 \left| r_2^I - h_2^2 x_k^I \right|^2 + h_2^2 \left| r_2^Q - h_1^2 x_k^Q \right|^2 \right\} \end{aligned} \tag{A.25}$$

where $\hat{x}_i$, h_i, r_i and x_k follow the definitions from (A.6). Note that the original received symbols, and not the equalised symbols, are used for detection. The ML decision criterion has remained the same; it is merely the signal set to which the criterion is applied that has been reduced, along with the addition of the first equalization and selection phase.

5. Numerical Results and Simulations

Presented in this section are numerical results based on the union bound, NN approximation and the new MDLB, all validated through simulation. The SER performance of the new simplified detection scheme is also compared with that of optimal ML detection. As shown in [5], the optimum rotation angle for both 4-QAM and 16-QAM with a single receive antenna is $31.7°$. This rotation angle is used here in all analyses since, as discovered through simulation, the optimum angle for $N \geq 3$ (where N is the number of relays) does not result in a significantly different SER. Simulations are performed over i.i.d flat fading Rayleigh channels with AWGN as described in Section 2 using 4-QAM and 16-QAM modulation. Simulation with 64-QAM modulation is also included for simplified detection with multiple receive antennas. We assume that full CSI for all channels is available at the receiver, that the receive antennas are spaced far enough apart to avoid correlation, and that all systems contain only a single transmit antenna. Since SER vs. rotation angle performance is mirrored horizontally along the $45°$ line, analysis is restricted to the range $0°$-$45°$.

5.1 Single Antenna Reception

We initially analyse SER performance for a system with a single receive antenna. Figure A.5 plots simulation results against the conventional union bound, the NN approximation and the

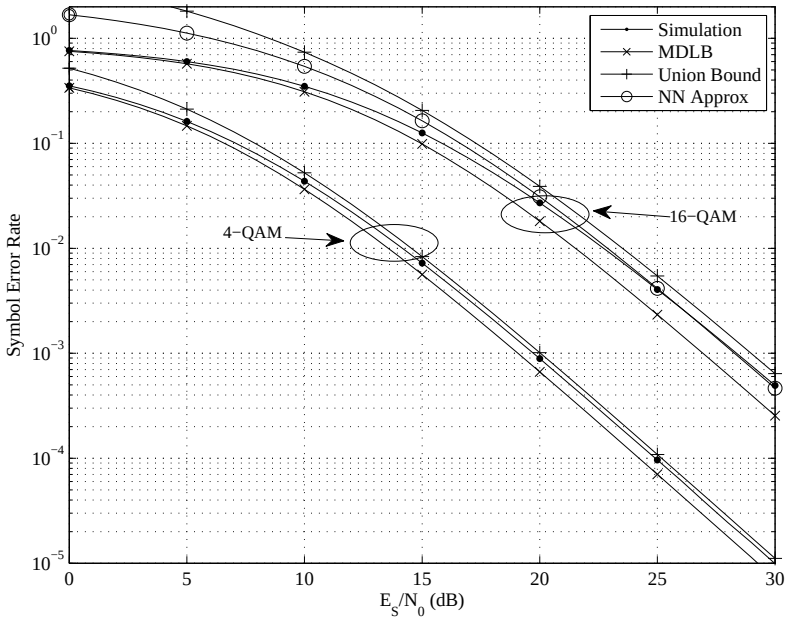

Figure A.5: SER of SSD system with $N = 1$

new MDLB for both 4-QAM and 16-QAM modulation. The NN approximation is identical to the union bound for 4-QAM and hence is not shown. The new MDLB, while the most accurate at low SNR (below 10dB), is not as tight as the union bound/NN approximation at high SNR at the chosen rotation angle. The NN approximation manages better SER performance than the union bound across the entire SNR range and hence is a better method for approximating the SER. All bounds show better SER performance with a smaller signal set and achieve full diversity.

As shown in [8], the optimum rotation angle for a system with MRC at the receiver is dependent on the number of receive antennas. It also varies for systems employing coding [14], and for cooperative SSD [18]. It is therefore of interest to determine the error performance of the derived performance bounds relative to the angle of rotation. The SER of the single receive antenna system is plotted against rotation angle in Figure A.6 at an SNR of 25dB, well into the high SNR region for both modulation schemes. Inspection of Figure A.6 reveals that the new MDLB is tight for the angles between 4° and 24° for 4-QAM and 8° and 20° for 16-QAM, making it suitable for error performance evaluation in systems using rotation angles in the mentioned ranges. Clearly, the NN approximation seems to switch between upper and lower bounding the error probability depending on the rotation angle for 16-QAM; however it does remain fairly tight throughout the rotation angle range. Figure A.6 visually corroborates the findings in [5]: the optimum rotation angle, defined as the angle at which the SER is a minimum, is approximately 31.7° for both 4-QAM and 16-QAM when $N = 1$.

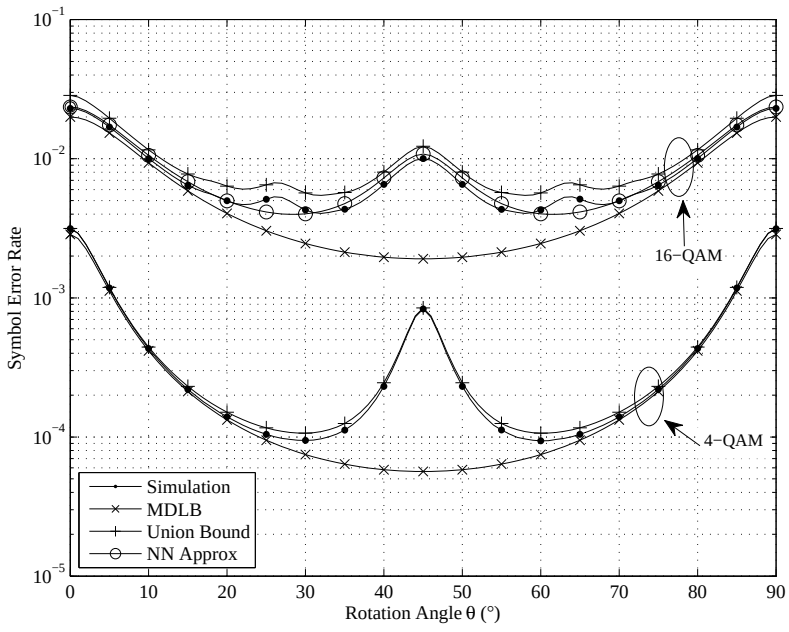

Figure A.6: SER vs. rotation angle at 25dB and $N = 1$

Figure A.7 plots the SER of the simplified detection scheme for single antenna reception. The simplified detection scheme appears to lose diversity with single antenna reception, yet SER performance is still better than conventional modulation by approximately 7dB at an SER of 10^{-3} for 4-QAM and approximately 4dB at an SER of 10^{-2} for 16-QAM when the number of searches is equal to $m = 3$ and $m = 5$ respectively. Increasing m to 9 brings further performance gains for 16-QAM; the improvement in complexity is worth the slight performance trade-off (approximately 1dB at 10^{-3}) when using 16-QAM and $m = 9$ as compared to conventional SSD detection.

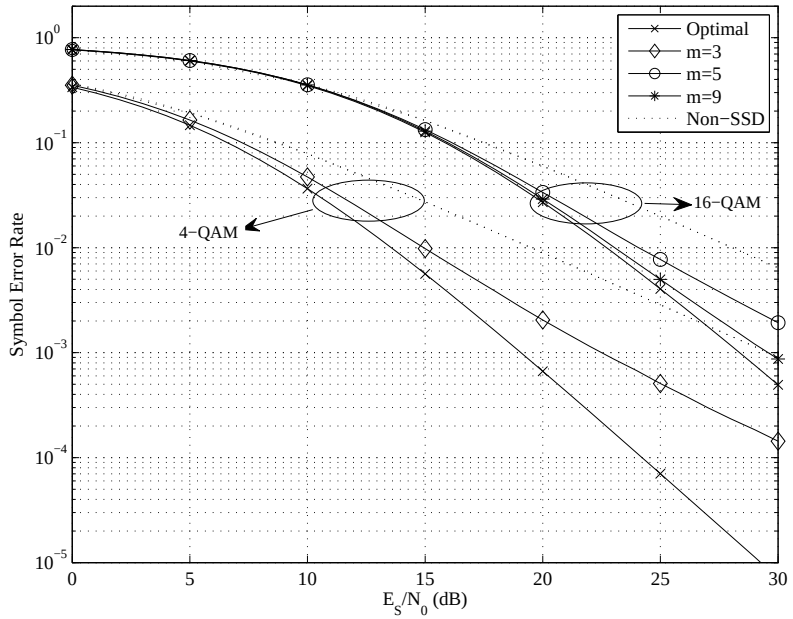

Figure A.7: SER of simplified SSD detection scheme with $N = 1$

5.2 Multiple Antenna Reception with MRC

We now consider performance of a system containing multiple receive antennas. The SER of the NN approximation and the new MDLB are plotted against simulation results in Figure A.8 for $N = 3$ and $N = 4$ receive antennas and MRC reception. The new MDLB, while not as tight as the NN approximation in the high SNR region, is far more accurate in the low SNR region and tight enough across the SNR range for the evaluation of SER performance in systems containing multiple receive antennas.

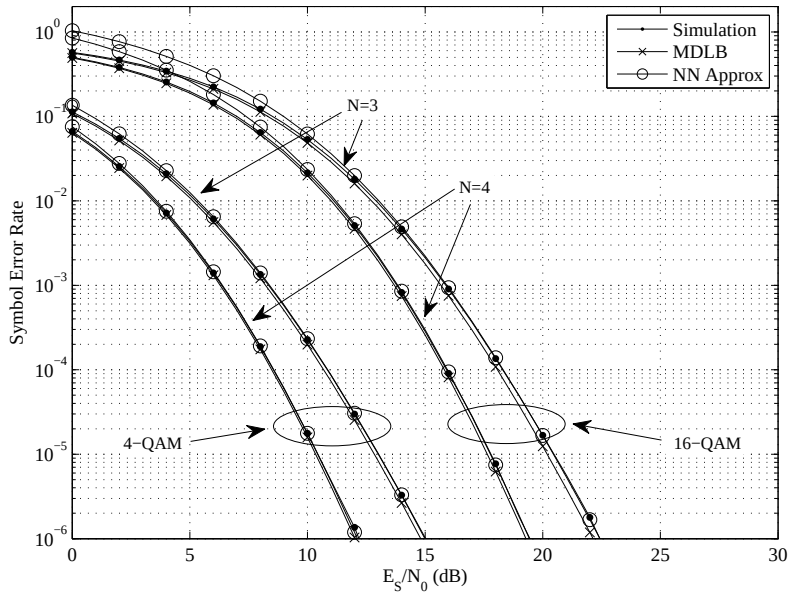

Figure A.8: SER of multiple receive antenna SSD system with MRC reception

Figure A.9 plots SER against rotation angle for the NN approximation and the MDLB at 10dB for 4-QAM and 15dB for 16-QAM with $N = 3$ receive antennas. The NN approximation is clearly tighter than the MDLB since the system is well into the high SNR region for both modulations. The MDLB, however, manages to be tight for a wide range of rotation angles: between 4° and 28° for 4-QAM and between 8° and 24° for 16-QAM. Even though the MDLB

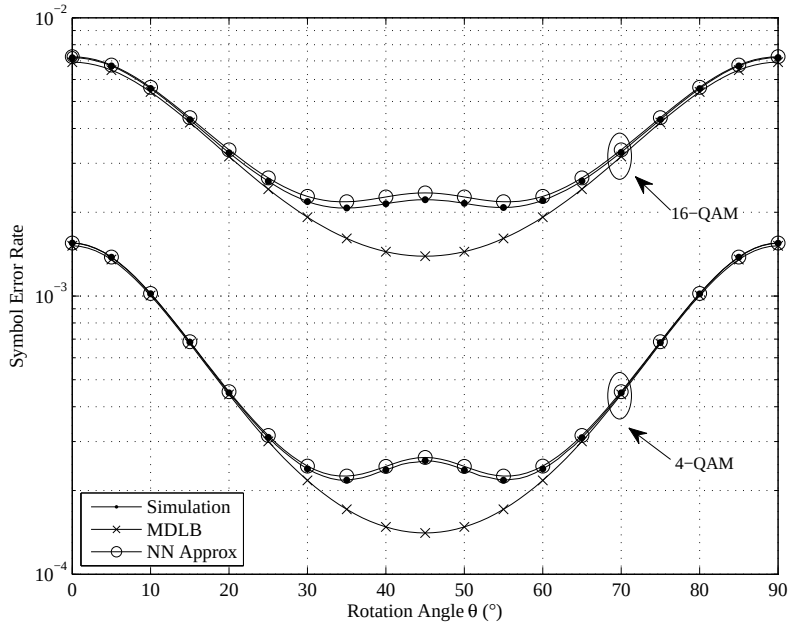

Figure A.9: SER vs. rotation angle with $N = 3$

appears to only be tight for the mentioned rotation angles as shown in Figure A.9, it is suitable for SER evaluation in multiple receive antenna systems as shown in Figure A.8. Comparing Figure A.5 and Figure A.8, it is clear that the MDLB achieves tighter performance across the SNR range when $N \geq 3$ compared to $N = 1$, and comparing Figure A.6 and Figure A.9 shows that the MDLB achieves tighter performance across a wider rotation angle range when $N = 3$ compared to $N = 1$.

Figure A.10 plots the SER of the simplified detection scheme for $N = 3$ and $N = 4$ receive antennas. SER performance in all cases is close to indistinguishable from the optimal detection scheme. Thus, in a system with multiple receive antennas, the simplified detection scheme is able to achieve very close to optimal detection SER performance with greatly reduced complexity compared to the optimal detection scheme. This is achieved for both $N = 3$ and $N = 4$ with 4-QAM when $m = 3$; however with 16-QAM and 64-QAM, $m = 5$ can only achieve close to optimal SER performance when $N = 4$, $m = 9$ is required when $N = 3$. Increasing the number of receive antennas results in a larger received SNR; enabling the value of m to be reduced since the received symbols have a higher probability of being closer in Euclidean distance to the transmitted symbols.

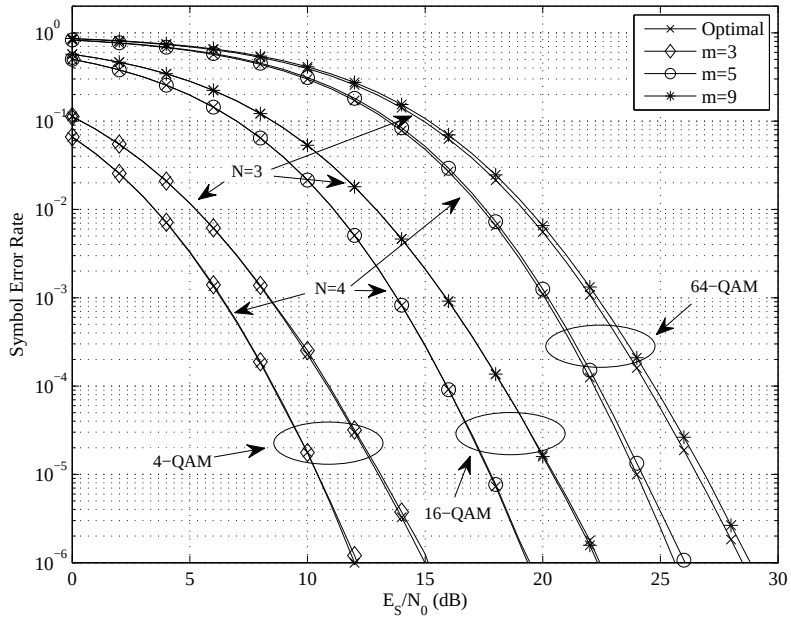

Figure A.10: SER of simplified SSD detection scheme with multiple receive antennas and MRC

Finally, we compare the complexity reduction achieved by the simplified detection scheme in Table A.1 in terms of the average number of searches needed in a given M-QAM constellation

for a given value of m. For the optimal ML detection scheme, the number of searches is the same for any point in the constellation. However, for the simplified detection scheme the number of searches is dependent on the location of symbol v, we thus compute the average number of searches required for a given M-QAM constellation size. The percentage reduction achieved is given by:

$$\% = \frac{opt - simp}{opt} \times 100 \tag{A.26}$$

where opt refers to the number of searches needed for optimal ML detection and $simp$ refers to the average number of searches needed for the simplified detection scheme. The 4-QAM constellation does not see much of a complexity decrease due to the small constellation size, however moving to 16-QAM and 64-QAM reduces the complexity substantially by up to 75% and 93% respectively.

For 4-QAM, the achieved SER for simplified detection with single antenna reception is in between non-SSD transmission and optimal detection while giving a complexity reduction of 25%. However, with multiple receive antennas, SER performance is close to indistinguishable from optimal detection with only 3 searches required. For 16-QAM, m can be reduced to 5 when $N = 4$ and reduced to 9 when $N = 3$, resulting in complexity reductions of 75% and 61% respectively. Close to optimal SER performance can be achieved using simplified detection with $m = 9$, 16-QAM, and a single receive antenna (up to 1dB at an error rate of 10^{-3}). This results in a complexity reduction of 61%, however diversity from SSD is lost. Finally, similar to 16-QAM, m can be reduced to 5 when $N = 4$ and reduced to 9 when $N = 3$, resulting in complexity reductions of 93% and 88% respectively for 64-QAM with multiple receive antennas. With all modulation schemes, increasing the number of receive antennas improves the SER performance of the simplified detection scheme and brings SER performance closer to that of optimal detection.

Table A.1: Average number of searches for given value of m and corresponding average complexity reduction percentage

	4-QAM		16-QAM		64-QAM	
	Avg.	%	Avg.	%	Avg.	%
Optimal ML	4	100%	16	100%	64	100%
$m = 3$	3	25%	-	-	-	-
$m = 5$	-	-	4	75%	4.5	93%
$m = 9$	-	-	6.25	61%	7.56	88%

6. Conclusion

SER performance of an SSD system employing a single transmit antenna and N receive antennas with MRC reception was presented. The union bound and the NN approximation were presented in closed form along with a new lower bound based on the minimum Euclidean distance (MDLB) of a rotated constellation. This was also presented in closed form. It was found that the NN approximation exhibits tighter SER performance than the union bound across most of the rotation angle range, and that the new MDLB exhibits tighter low SNR performance than the upper bounds, yet is looser than the upper bounds at high SNR and angles closer to the optimum when $N = 1$. However, when $N \geq 3$, SER performance of the MDLB is tight across the SNR range. The MDLB is simple to compute and only requires a change in variable to evaluate SSD in other systems if the conventional M-QAM conditional SER is used.

A simplified detection scheme for SSD systems was also presented and compared to the optimal detection scheme using simulation. It was found that the simplified detection scheme loses diversity when $N = 1$, however SER performance is still significantly better than non-SSD transmission and improves with increasing values of m. With $N = 3$, SER performance is close to indistinguishable from optimal detection for 4-QAM, 16-QAM and 64-QAM with complexity reductions of 25%, 61% and 88% respectively; and with $N = 4$, of 25%, 75% and 93% respectively.

7. References

[1] T. Eng, N. Kong, and L. B. Milstein, "Comparison of diversity combining techniques for Rayleigh-fading channels," *IEEE Trans. Commun.*, vol. 44, no. 9, pp. 1117–1129, Sep. 1996.

[2] L. Zheng and D. N. C. Tse, "Diversity and multiplexing: A fundamental tradeoff in multiple-antenna channels," *IEEE Trans. Inf. Theory*, vol. 49, no. 5, pp. 1073–1096, May 2003.

[3] J. Boutros and E. Viterbo, "Signal space diversity: A power- and bandwidth-efficient diversity technique for the Rayleigh fading channel," *IEEE Trans. Inf. Theory*, vol. 44, no. 4, pp. 1453–1467, Jul. 1998.

[4] *Frame structure channel coding and modulation for a second generation digital terrestrial television broadcasting system (DVB-T2)*, European Standard, ETSI EN 302 755, Sep. 2009.

[5] G. Taricco and E. Viterbo, "Performance of component interleaved signal sets for fading channels," *IEE Electronics Letters*, vol. 32, no. 13, pp. 1170–1172, Apr. 1996.

[6] N. F. Kiyani, J. H. Weber, A. G. Zajic, and G. L. Stuber, "Performance analysis of a system using coordinate interleaving and constellation rotation in Rayleigh fading channels," in *Proc. IEEE 68th Vehicular Technology Conf.*, 2008, pp. 1–5.

[7] J.-C. Belfiore and E. Viterbo, "Approximating the error probability for the independent Rayleigh fading channel," in *Proc. Int. Symp. Information Theory*, 2005, pp. 362–362.

[8] S. Jeon, I. Kyung, and M.-S. Kim, "Component-interleaved receive MRC with rotated constellation for signal space diversity," in *IEEE 70th Vehicular Technology Conf. Fall*, 2009, pp. 1–6.

[9] J. Kim and I. Lee, "Analysis of symbol error rates for signal space diversity in Rayleigh fading channels," in *Proc. IEEE Int. Conf. on Communications*, 2008, pp. 4621–4625.

[10] J. Kim, W. Lee, J.-K. Kim, and I. Lee, "On the symbol error rates for signal space diversity schemes over a Rician fading channel," *IEEE Trans. Commun.*, vol. 57, no. 8, pp. 2204–2209, Aug. 2009.

[11] A. G. I. Fabregas and E. Viterbo, "Sphere lower bound for rotated lattice constellations in fading channels," *IEEE Trans. Wireless Commun.*, vol. 7, no. 3, pp. 825–830, Mar. 2008.

[12] S. B. Slimane, “An improved PSK scheme for fading channels,” *IEEE Trans. Veh. Technol.*, vol. 47, no. 2, pp. 703–710, May 1998.

[13] R. Ying and M. Z. Wang, “Performance analysis of full-rate STBCs from coordinate interleaved orthogonal designs,” in *IEEE Int. Conf. on Communications*, 2007, pp. 4610–4615.

[14] M. Z. A. Khan and B. S. Rajan, “Single-symbol maximum likelihood decodable linear STBCs,” *IEEE Trans. Inf. Theory*, vol. 52, no. 5, pp. 2062–2091, May 2006.

[15] H. Xu, “Symbol error probability for generalized selection combining reception of M-QAM,” *SAIEE Africa Research Journal*, vol. 100, no. 3, pp. 68–71, Sep. 2009.

[16] J. G. Proakis and M. Salehi, *Digital Communications*, 5th ed. McGraw-Hill, 2008.

[17] M. K. Simon and M. S. Alouini, *Digital Communication Over Fading Channels*, 2nd ed. Wiley-IEEE Press, 2005.

[18] S. A. Ahmadzadeh, S. A. Motahari, and A. K. Khandani, “Signal space cooperative communication,” *IEEE Trans. Wireless Commun.*, vol. 9, no. 4, pp. 1266–1271, Apr. 2010.

Paper B

Distributed Switch and Stay Combining with Partial Relay Selection and Signal Space Diversity

Z. Paruk and H. Xu

Prepared for submission to IET Communications Journal.

Abstract

Spatial diversity schemes are often used to extract additional performance from wireless communication systems. Combining a distributed switch and stay combining (DSSC) cooperative communication network with the partial relay selection (PRS) protocol gives the benefit of diversity while simplifying hardware, processing and feedback requirements. Since only a single relay is ever active, the destination employs no combiner and the best relay is chosen based on first hop relay conditions; however achieved performance is worse than other distributed protocols such as distributed selection combining (DSC). In this study, signal space diversity (SSD) is added to the DSSC-PRS system to provide further diversity and error performance gains at the expense of necessitating a maximum-likelihood (ML) detector with increased complexity at the receiver. Analytical results are presented in the form of a lower bound based on the minimum distance lower bound (MDLB) for SSD systems and are verified with simulation. The DSSC-PRS-SSD system shows an improvement of 5dB at a symbol error rate (SER) of 10^{-4} and a clear diversity order improvement. Spectral efficiency of the new system with SSD is slightly decreased at low signal-to-noise ratio (SNR), but is still an improvement over other distributed schemes such as DSC.

1. Introduction

Diversity is an often used method of extracting additional performance from wireless communication systems. Most often, space or time diversity is exploited to provide performance gains. Classical spatial diversity schemes involve combining multiple copies of a signal received over independent paths, usually multiple antennas, to give a signal with significantly better signal-to-noise ratio (SNR) [1]. Cooperative communication has also been proposed [2] to exploit the inherent diversity present in a multi-user cooperative system by retransmitting signals received by a 'relay' node to the destination node, thereby creating another independent channel. Further, signal space diversity (SSD) has been proposed [3] which exploits the diversity present in the different dimensions of a multi-dimensional signal set by ensuring that the different dimensions are affected by independent fading through the interleaving of the in-phase and quadrature components of a symbol pair.

In an N relay cooperative system employing all N relays to forward signals, throughput is adversely affected as N gets large due to the time division multiple access (TDMA) time slot allocation per relay [4]. In [5], a relay selection scheme for amplify-and-forward (AF) relays was proposed that chooses only a single relay for re-transmission, namely the 'best' relay based on the two-hop channel conditions. The proposed relay selection scheme (distributed selection combining or DSC) achieves full diversity of $N + 1$ for N relays.

Diversity order analysis of cooperative decode-and-forward (DF) networks employing relay selection was conducted in [6]. It was found that full diversity is also achievable with N DF relays using the appropriate combining at the destination and relay selection. Selecting only a single relay for retransmission achieves higher spectral efficiency when compared to N retransmitting relays [5, 6], however feedback requirements are high. In addition, while relay selection schemes offer higher spectral efficiency than N relay forwarding schemes, spectral efficiency can still be improved further.

Switch and stay combining (SSC) is another efficient diversity exploiting scheme that switches between signals from two branches based on their instantaneous received SNR. SSC is an improvement over selection combing (SC) since the frequency of branch switching is reduced, lowering switching losses, although some error performance is sacrificed [7]. In [8], a 'virtual' antenna array was created consisting of the 'relayed' and 'direct' branches: the relayed branch comprising of a single DF relay and the direct branch comprising of the source node. It was found that full diversity was achievable with a single relay with higher spectral efficiency compared to relay selection schemes.

Two relays were considered for a distributed switch and stay combining (DSSC) network in [9], however messages only arrive at the destination via either relay and not the source directly. Partial relay selection (PRS) was proposed in [10] for amplify-and-forward (AF) relays enabling multiple relays to form part of a cooperative network, with only a single relay chosen to forward messages entirely by its first-hop SNR. This negates the need for overhead inducing feedback from the destination for relay selection. Instead, the relays communicate with the source to determine the best relay for communication if the relayed link is active. In [10], signals arrive at the destination only via the relays and not via the source, providing no additional diversity from cooperation.

In [11], the DSSC system was extended to a network comprising of N DF relays with the best relay selected according to the PRS protocol, along with a signal path from the source to the destination. It was found that diversity up to an order of two was therefore achievable, however, due to PRS, increasing the number of relays beyond $N = 3$ does not result in any further improvements in error performance. The DSSC-PRS system thus provides a low complexity cooperative network with high spectral efficiency; however, error performance and diversity can be improved further.

In this study, we propose the addition of SSD to a DSSC-PRS system to enable further diversity and error performance gains while making no changes to the configuration of the cooperative network. The addition of SSD merely adds a more complex maximum-likelihood (ML) detector at the relays and destination, since all nodes participate in the SSD protocol. SSD achieves the additional diversity and error performance gains without any additional bandwidth, hardware or transmit power requirements. Thus, the low complexity of the DSSC-PRS system is maintained while bringing additional performance gains. Signal space cooperative communication was also proposed in [12], however in that work diversity from both cooperation and SSD was not achieved. In [13], SSD was added to a coded DF cooperative network, however no performance analysis was given.

Symbol error rate (SER) performance will be evaluated using the minimum distance lower bound (MDLB) proposed in [14] and compared with simulation results. Variances in channel conditions between the source, relays and the destination will also be investigated as well as the spectral efficiency of the new system. The rest of this paper is organized as follows: Section 2 presents the system model, Section 3 presents performance analysis, Section 4 presents results and Section 5 presents concluding remarks.

2. System Model

Consider a cooperative communication network comprising of $N + 2$ total nodes. The source node is termed S, the N relay nodes are termed R_i with i being the relay index, and the destination node is termed D. Each node contains a single transmit/receive antenna. Communication occurs in a half-duplex fashion, i.e. nodes cannot transmit and receive at the same time. M-QAM modulation with SSD is used between all nodes. The network can be visualized in Figure B.1.

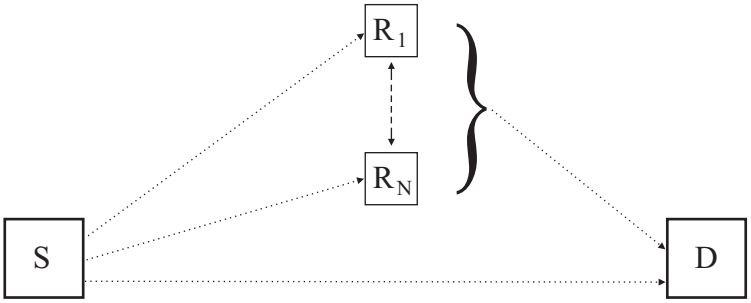

Figure B.1: Typical distributed switch and stay combining network with N relays

As shown in Figure B.1, a DSSC network [8] is so named because of the switching between the direct path (termed $\mathfrak{D}$) from the source to the destination, and the relayed path (termed $\mathfrak{R}$) created between the source, ith relay and the destination (the $S - R_i - D$ path). Only a single relay ever communicates with the destination at any time. The two mentioned paths form the virtual branches of the DSSC network.

Following the standard SSC scheme operation, the destination chooses to either stay with the current branch for reception or switch to the other branch; this switching occurs when the currently selected branch instantaneous SNR falls below a threshold. The threshold, denoted γ_T, can be entirely pre-determined according to the network topology and modulation method employed and thus saves the selecting node from performing costly calculations to determine the optimal threshold. The destination, therefore, employs no combiner.

The forwarding relay is chosen by the PRS protocol [10]. With PRS, the relay with the largest first-hop SNR is chosen to relay messages during the second hop if the relayed link is currently active. This ensures that the number of branches in the network is restricted to two; a necessary constraint since SSC does not offer any diversity or error performance improvement when the number of identically distributed branches is greater than two [7].

We assume quasi-static flat fading channels between all nodes ($S-D$, $S-R_i$, and R_i-D) i.e. the fading is constant over a block of SSD symbols referred to as SSD$_j$ in Figure B.2, where j is the SSD time segment index, explained further in this section. It is also assumed that detection is performed after the removal of the phase shift induced by fading. Thus the fading is modelled as a Rayleigh distributed random variable with amplitude distributed according to $f_h\left(h_{p,j}\right) = \frac{h_{p,j}}{\sigma^2} \exp\left(\frac{-h_{p,j}^2}{2\sigma^2}\right)$ where p refers to the signal path ($S-D$, $S-R_i$, and R_i-D). The fading has unit second moment, i.e. $E\left[h_{p,j}^2\right] = 2\sigma^2 = 1$. The transmitted signals are perturbed by additive white Gaussian noise (AWGN), modelled as a circular symmetric Gaussian random variable with distribution $n_{p,j} \sim \mathcal{CN}\left(0, N_0\right)$, i.e. zero mean and variance $N_0/2$ per dimension. We further assume that the relays are grouped into clusters, with an entire cluster of relay nodes chosen to participate in the communication based on favourable channel conditions. This assumption grants the relays the property of shared average channel characteristics [11].

Similar to [11], transmission occurs in two phases: the broadcast phase and the relay phase. In the broadcast phase the source transmits a message block to all participating nodes in the network, i.e. all relay nodes and the destination node. During the relay phase, if the relayed branch is active, a single relay from N (chosen by partial relay selection, i.e. the relay with the highest first-hop SNR) retransmits to the destination. The chosen relay node employs the well-studied uncoded DF processing protocol, i.e. it fully detects the signal received in the broadcast phase and thereafter re-modulates and retransmits during the relay phase. The two phases are assumed to be two time slots in this system.

The transmission protocol presented in [11] has been modified due to the addition of SSD. The time slots for individual phases are now split into two time segments to facilitate the transmission of SSD symbol pairs. Figure B.2 visualizes the time slot arrangement for the four possible cases arising due to the addition of SSD, contrasting with the two cases possible for the non-SSD system. In each case, the instantaneous SNR of the link is determined via pilot symbols transmitted during a training period at the beginning of each SSD time segment as indicated in the figure. Defining the active link to be the link chosen by the destination for reception during the previous time slot, the four cases can be briefly described as follows:

- Case 1: The direct link is active ($\mathfrak{D}$) and the destination chooses to stay with the direct link ($\mathfrak{D}$) for reception. Maximum spectral efficiency is obtained with this case since there is no need for messages to be relayed.

- Case 2: The direct link is active ($\mathfrak{D}$) and the relayed link ($\mathfrak{R}$) is chosen for reception. Thus the relay phase is required and the destination uses the signals received during the relay phase only.
- Case 3: The relayed link is active ($\mathfrak{R}$) and the relayed link ($\mathfrak{R}$) is chosen for reception. Again the relay phase is required.
- Case 4: The relayed link is active ($\mathfrak{R}$) and the destination chooses the direct link for reception ($\mathfrak{D}$). In this case, a single SSD symbol block (with pilot symbols) needs to be transmitted during the first SSD time segment along with pilot symbols during the second SSD time segment training period before the destination is able to make a decision about the quality of the relayed link. This is necessary since it decides based on the minimum of the two SSD time segment SNRs (explained further in this section). This symbol block is subsequently discarded, resulting in spectral efficiency loss.

We assume perfect feedback channels between the relays and the source for the purpose of choosing the best relay according to the PRS protocol, and between the destination and relays/source for informing them of branch switching in all outlined cases.

In Figure B.2, the subscript j in SSD_j refers to the SSD symbol block transmitted in time segment j.

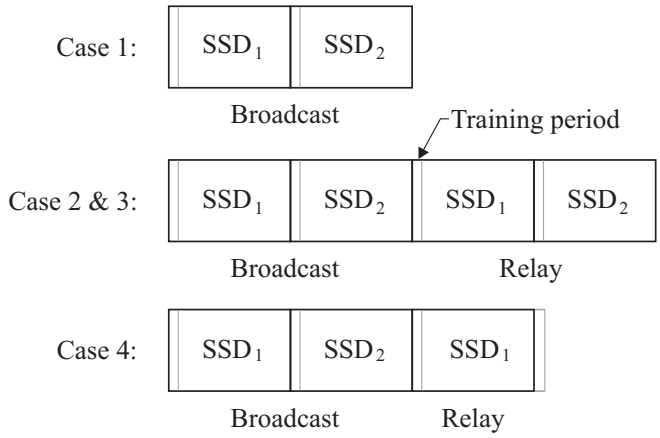

Figure B.2: Time slot arrangement for a DSSC-PRS network with SSD

Transmission of SSD symbols occurs according to the following procedure: The source node maps incoming data bits to symbols chosen from a constellation $\tilde{S}$ which has been rotated by an angle θ to give rotated symbols x. The rotated symbols x are then arbitrarily grouped into pairs and component interleaved to give symbols u. The interleaved symbols are then split between the two SSD time segments, i.e. all of the first symbols in a symbol pair are

denoted u_1 and transmitted in SSD time segment 1, and the second symbols of a symbol pair are denoted u_2 and transmitted in SSD time segment 2 of the broadcast phase. The received symbols at the relays and the destination during either time segment in the broadcast phase can then be written:

$$\begin{aligned} r_{SR_i,j} &= h_{SR_i,j}u_j + n_{SR_i,j} \\ r_{SD,j} &= h_{SD,j}u_j + n_{SD,j} \end{aligned} \tag{B.1}$$

where $i \in \{1, ..., N\}$ is the relay index, $j \in \{1, 2\}$ is the SSD time segment index and $r_{p,j}$ is the received signal from path p during time segment j. If the direct branch $\mathfrak{D}$ is currently active, the relays do not participate any further in the current symbol transmission and the destination performs detection of the symbols received during the broadcast phase. If the relayed branch $\mathfrak{R}$ is currently active, the pre-selected relay (denoted with index l) then performs detection of the received SSD symbols to give symbols $\hat{u}_j$, which are then re-transmitted to the destination during the relay phase. The received symbols at the destination during either time segment of the relay phase can then be written:

$$r_{R_lD,j} = h_{R_lD,j}\hat{u}_j + n_{R_lD,j} \tag{B.2}$$

where l is the chosen relay index and j is the SSD time segment index. We assume that full CSI is available at all nodes for the purposes of SSD detection.

The utilization of SSD necessitates the arrival of symbols from both SSD time segments at each participating node before detection can be performed. Thus, the problem of which time segment instantaneous SNR to choose to maximise error performance presents itself. In [15], it has been shown that the equivalent two-hop instantaneous SNR γ_{eq} of a cooperative communication system is upper bounded by the minimum of the two single-hop instantaneous SNRs; and that the subsequent error rate approximated using the equivalent two-hop distribution is asymptotically tight in the high SNR region. It is further shown [15] that a system using the equivalent SNR to represent the dual-hop SNR achieves full diversity regardless of modulation. Analogously, we propose that the minimum of the instantaneous SNRs across the two SSD time segments be chosen to represent the instantaneous channel SNR during both time segments. Thus the equivalent SNR across the SSD time segments can be expressed as:

$$\gamma_{SSD} = \min(\gamma_1, \gamma_2) \tag{B.3}$$

where γ_1 and γ_2 are the instantaneous SNRs of the respective SSD time segments. Detection of the SSD symbols after the arrival of a symbol pair is performed in the ML sense, and it is here that the increase in system complexity is introduced. The ML rule for both symbols in a symbol pair can be written after de-interleaving, for any path p, as:

$$\begin{aligned}\hat{x}_1 &= \arg\min_{x_k \in \tilde{S}} \left\{ \left| r_{p,1}^I - h_{p,1} x_k^I \right|^2 + \left| r_{p,1}^Q - h_{p,2} x_k^Q \right|^2 \right\} \\ \hat{x}_2 &= \arg\min_{x_k \in \tilde{S}} \left\{ \left| r_{p,2}^I - h_{p,2} x_k^I \right|^2 + \left| r_{p,2}^Q - h_{p,1} x_k^Q \right|^2 \right\}\end{aligned} \tag{B.4}$$

where $\hat{x}_j$ are the detected symbols, $r_{p,j}$ are the received symbols, $h_{p,j}$ are the fading coefficients, j indicates the SSD time segment, and $k \in \{1, ..., M\}$, where M denotes the cardinality of the constellation. The operations $(\cdot)^I$ and $(\cdot)^Q$ refer to the in-phase and quadrature components of a signal respectively.

3. Performance Analysis

For convenient discussion, we use $f(x)$ to denote the PDF of random variable x, $F(x)$ to denote its CDF, and $P(z)$ to denote the probability of event z.

The minimum of the instantaneous received SNRs between the two SSD time segments is needed for best relay selection and for branch switching. The following expression given in [16] can be used to find the instantaneous SNR between the two SSD time segments, which we term the decision SNR:

$$\omega = \min(x, y) = \begin{cases} y & x > y \\ x & x \leq y \end{cases} \tag{B.5}$$

We can then write the following expression:

$$\begin{aligned} F_\omega(\omega) &= P\{\min(x, y) \leq \omega\} = P\{y \leq \omega, x > y\} + P\{x \leq \omega, x \leq y\} \\ &= 1 - P\{w > \omega\} = 1 - P\{x > \omega, y > \omega\} \\ &= F_x(\omega) + F_y(\omega) - F_{x,y}(\omega, \omega) \end{aligned} \tag{B.6}$$

Assuming that the random variables are independent, (B.6) can be differentiated to give an expression for the PDF of the minimum of two random variables:

$$f_\omega(\omega) = f_x(\omega) + f_y(\omega) - f_x(\omega) F_y(\omega) - F_x(\omega) f_y(\omega) \tag{B.7}$$

Where $f_x(\omega)$ and $f_y(\omega)$ are the PDF's of the two independent variables. Substituting the exponential (chi-square with two-degrees of freedom) distributions representing the SNR for a given Rayleigh fading channel and performing some straightforward manipulation gives the following, also shown in [11]:

$$f_{\gamma_{SSD}}(\gamma) = \frac{1}{\kappa_p} \exp\left(\frac{-\gamma}{\kappa_p}\right) \tag{B.8}$$

where γ is the new decision SNR and the new variable $\kappa_p = (1/\overline{\gamma}_1 + 1/\overline{\gamma}_2)^{-1}$ now represents the average decision SNR over both SSD time segments, given that $\overline{\gamma}_j$ is the average channel SNR during SSD time segment j. Having assumed that the average channel SNR remains the same during both SSD time segments, the average decision SNR becomes $\kappa_p = \overline{\gamma}_p/2$, where $\overline{\gamma}_p$ is the average SNR of the channel over a given path p ($S-D$, $S-R$ or $R-D$). We term this decision PDF $f_{\gamma_{SSD}}(\gamma)$. Note that the minimum of any number of exponentially distributed

random variables is still exponentially distributed, with a change in expectation. Integrating the PDF in (B.8) gives the decision CDF:

$$F_{\gamma_{SSD}}(\gamma) = 1 - \exp\left(\frac{-\gamma}{\kappa_p}\right) \tag{B.9}$$

It is important to note that the presented decision PDF and CDF and the corresponding decision SNR will be used only to determine the steady state branch selection probabilities, the probability of branch switching, and for best relay selection, but not for the probability of error since the receiving nodes use symbols from both time slots (as opposed to the minimum as suggested by the PDF) when detecting received symbols.

Following the PRS protocol given in section 2, the relay with the best instantaneous first-hop SNR is chosen for re-transmission if the relayed branch is currently active. Defining the instantaneous SNR from the source to the best relay to be γ_{SR}, the desired SNR can then be expressed as:

$$\gamma_{SR} = \max\left(\gamma_{SR_1}, \gamma_{SR_2}, ..., \gamma_{SR_N}\right) \tag{B.10}$$

where γ_{SR_i} denotes the SNR between the source and relay i as defined in the system model, and now with PDF $f_{\gamma_{SR_i}}(\gamma)$ distributed according to (B.8) and CDF $F_{\gamma_{SR_i}}(\gamma)$ distributed according to (B.9). From [16], we know that the CDF of the maximum of two independent random variables can be found by multiplying their respective CDF's, i.e. the CDF of $z = \max(x, y)$ can be written $F(z) = F(x)F(y)$; we can therefore write, using the binomial expansion [11]:

$$F_{\gamma_{SR}}(\gamma) = \left[F_{\gamma_{SR_i}}(\gamma)\right]^N = \sum_{i=1}^{N} \binom{N}{i} (-1)^{i+1} \left(1 - \exp\left(\frac{-i\gamma}{\kappa_{SR}}\right)\right) \tag{B.11}$$

where $\kappa_{SR} = \overline{\gamma}_{SR}/2$ now represents the average decision SNR of the link between the source and the best relay. Taking the derivative of the CDF in (B.11) gives the PDF:

$$f_{\gamma_{SR}}(\gamma) = \sum_{i=1}^{N} \binom{N}{i} (-1)^{i+1} \frac{i}{\kappa_{SR}} \exp\left(\frac{-i\gamma}{\kappa_{SR}}\right) \tag{B.12}$$

The path between the best relay and the destination node with decision SNR denoted γ_{RD} follows a simple exponential distribution as defined in (B.8) and (B.9), with PDF and CDF [11]:

$$f_{\gamma_{RD}}(\gamma) = \frac{1}{\kappa_{RD}} \exp\left(\frac{-\gamma}{\kappa_{RD}}\right) \tag{B.13}$$

$$F_{\gamma_{RD}}(\gamma) = 1 - \exp\left(\frac{-\gamma}{\kappa_{RD}}\right) \tag{B.14}$$

With $\kappa_{RD} = \overline{\gamma}_{RD}/2$ representing the average decision SNR between the best relay and the destination. Again making use of Property 1 from [15], the dual-hop SNR, i.e. the SNR of the relayed link $\gamma_{\mathfrak{R}}$, can be approximated by the minimum of the two single-hop SNRs found previously:

$$\gamma_{\mathfrak{R}} = \min(\gamma_{SR}, \gamma_{RD}) \tag{B.15}$$

Making use of (B.7) and substituting (B.11), (B.12), (B.13) and (B.14), the following expression for the PDF of $\gamma_{\mathfrak{R}}$ is easily obtainable:

$$f_{\gamma_{\mathfrak{R}}}(\gamma) = \sum_{i=1}^{N} \binom{N}{i} (-1)^{i+1} \frac{i}{\mu_i} \exp\left(\frac{-\gamma}{\mu_i}\right) \tag{B.16}$$

where μ_i is given by $\mu_i = (i/\kappa_{SR} + 1/\kappa_{RD})^{-1}$. The CDF of $\gamma_{\mathfrak{R}}$ is easily given by integrating the PDF from (B.16) to give:

$$F_{\gamma_{\mathfrak{R}}}(\gamma) = \int_0^{\gamma} f_{\gamma_{\mathfrak{R}}}(\gamma)\, d\gamma = \sum_{i=1}^{N} (-1)^{i-1} \binom{N}{i} \left(1 - \exp\left(\frac{-\gamma}{\mu_i}\right)\right) \tag{B.17}$$

The direct path (i.e. the path between the source and the destination nodes) SNR $\gamma_{\mathfrak{D}}$ is equivalent to γ_{SD}, with PDF and CDF distributed according to (B.8) and (B.9) respectively:

$$f_{\gamma_{\mathfrak{D}}}(\gamma) = \frac{1}{\kappa_{SD}} \exp\left(\frac{-\gamma}{\kappa_{SD}}\right) \tag{B.18}$$

$$F_{\gamma_{\mathfrak{D}}}(\gamma) = 1 - \exp\left(\frac{-\gamma}{\kappa_{SD}}\right) \tag{B.19}$$

where $\kappa_{SD} = \overline{\gamma}_{SD}/2$ now represents the average decision SNR of the link between the source and the destination. The steady state selection probabilities for the direct branch $\mathfrak{D}$ or the relayed branch $\mathfrak{R}$ can be derived by considering a two-state Markov chain [17]. Steady state analysis gives the following probabilities of branch selection, where $p_{\mathfrak{D}}$ and $p_{\mathfrak{R}}$ are the probabilities of the direct and relayed branch being active respectively:

$$
\begin{aligned}
p_{\mathfrak{D}} &= F_{\gamma_{\mathfrak{R}}}(\gamma_T) / \left[F_{\gamma_{\mathfrak{D}}}(\gamma_T) + F_{\gamma_{\mathfrak{R}}}(\gamma_T)\right] \\
p_{\mathfrak{R}} &= F_{\gamma_{\mathfrak{D}}}(\gamma_T) / \left[F_{\gamma_{\mathfrak{D}}}(\gamma_T) + F_{\gamma_{\mathfrak{R}}}(\gamma_T)\right]
\end{aligned}
\tag{B.20}
$$

These can easily be computed using the CDF's outlined previously in (B.19) and (B.17).

3.1 Symbol Error Probability

The SER is easily derived by considering the law of total probability. Assuming that the current branch is the direct branch ($\mathfrak{D}$), two possible cases arise: that of the current branch SNR being less than the threshold or the current branch SNR being greater the threshold, i.e. $\gamma_D < \gamma_T$ or $\gamma_D > \gamma_T$. Considering the symbol error probabilities for each of these cases individually, and repeating the process for the relayed branch, the symbol error probability for the DSSC-PRS-SSD system can be expressed as [8]:

$$
\begin{aligned}
P_S^{DSSC-PRS-SSD}(e) \geq\ & p_{\mathfrak{D}} \left[\begin{array}{l} \left(1 - F_{\gamma_{\mathfrak{D}}}(\gamma_T)\right) P\left(e \middle| \{\mathfrak{D}, \gamma_{\mathfrak{D}} > \gamma_T\}\right) + \\ F_{\gamma_{\mathfrak{D}}}(\gamma_T)\, P(e|\mathfrak{R}) \end{array} \right] + \\
& p_{\mathfrak{R}} \left[\begin{array}{l} \left(1 - F_{\gamma_{\mathfrak{R}}}(\gamma_T)\right) P\left(e \middle| \{\mathfrak{R}, \gamma_{\mathfrak{R}} > \gamma_T\}\right) + \\ F_{\gamma_{\mathfrak{R}}}(\gamma_T)\, P(e|\mathfrak{D}) \end{array} \right]
\end{aligned}
\tag{B.21}
$$

where the SER is lower bounded by the MDLB, shown in (B.27). The terms $F_{\gamma_{\mathfrak{D}}}(\gamma_T) P(e|\mathfrak{R})$ and $F_{\gamma_{\mathfrak{R}}}(\gamma_T) P(e|\mathfrak{D})$ are not conditioned upon the relevant instantaneous branch SNR because it does not matter; if a branch switch occurs the new branch is used regardless of its instantaneous SNR being above or below the threshold. For each of the following error cases, the average link SNR ($\overline{\gamma}_p$) is used with the relevant PDF and not the average decision SNR (κ_p).

The symbol error probability for the direct and relayed branches will be considered separately. It is convenient, however, to define an auxiliary function $I(\cdot)$ which will assist in simplifying the analytical expressions. We define the $I(\cdot)$ function as the integration of the conditional symbol error probability for a direct link from a threshold value z, specifying any square M-QAM as the modulation scheme and the exponential distribution to represent the SNR of a Rayleigh fading channel. We can then write:

$$
\begin{aligned}
I(a, b, c, z) &= \int_z^{\infty} P(e|\gamma)\, f_{\gamma}(\gamma)\, d\gamma \\
&= \int_z^{\infty} \left[4aQ\left(\sqrt{b\gamma}\right) - 4a^2 Q^2\left(\sqrt{b\gamma}\right)\right] \frac{1}{c} \exp\left(\frac{-\gamma}{c}\right) d\gamma
\end{aligned}
\tag{B.22}
$$

where the conditional symbol error probability $P\left(e|\gamma\right)$ is given in [18], the exponential distribution accepts any average c as a parameter, $a = \left(1 - \frac{1}{\sqrt{M}}\right)$ and $b = \frac{3}{M-1}$. Using the trapezoidal approximations to the $Q\left(\cdot\right)$ and $Q^2\left(\cdot\right)$ functions [19], the defined $I\left(\cdot\right)$ function integral can easily be solved and written as:

$$I\left(a,b,c,z\right) = \frac{a}{n}\left\{\alpha - \beta + (1-a)\sum_{d=1}^{n-1}\varepsilon + \sum_{d=1}^{2n-1}\varepsilon\right\} \tag{B.23}$$

where

$$\alpha = \frac{1}{2}\left(\frac{2}{b\overline{\gamma}+2}\right)\exp\left(-z\left[\frac{b\overline{\gamma}+2}{2\overline{\gamma}}\right]\right) \tag{B.24}$$

$$\beta = \frac{a}{2}\left(\frac{1}{b\overline{\gamma}+1}\right)\exp\left(-z\left[\frac{b\overline{\gamma}+1}{\overline{\gamma}}\right]\right) \tag{B.25}$$

$$\varepsilon = \left(\frac{S_d}{b\overline{\gamma}+S_d}\right)\exp\left(-z\left[\frac{b\overline{\gamma}+S_d}{\overline{\gamma}S_d}\right]\right) \tag{B.26}$$

and $S_d = 2\sin^2\left(d\pi/4n\right)$ and n is the total number of iterations used in the approximation. We now extend the $I\left(\cdot\right)$ function to consider the case of M-QAM with SSD modulation. Using SSD modulation, the defined $I\left(\cdot\right)$ function can be redefined using the MDLB presented in [14] to consider the independent fading on each dimension of the constellation and the rotation angle θ. Double integrating over the MDLB gives the $I_{SSD}\left(\cdot\right)$ function:

$$I_{SSD}\left(a,b,c,z,\theta\right) = \int_z^\infty\int_z^\infty\left[\begin{array}{l}4aQ\left(\sqrt{b\zeta}\right) - \\ 4a^2Q^2\left(\sqrt{b\zeta}\right)\end{array}\right]\left[\begin{array}{l}\frac{1}{c}\exp\left(\frac{-\gamma_1}{c}\right)\times \\ \frac{1}{c}\exp\left(\frac{-\gamma_2}{c}\right)\end{array}\right]d\gamma_1 d\gamma_2 \tag{B.27}$$

where $\zeta = \left(\gamma_1\cos^2\theta + \gamma_2\sin^2\theta\right)$, obtained by computing the minimum Euclidean distance of a rotated constellation with independent fading on the different dimensions. Performing the integration in (B.27) gives a lower bound which can be directly substituted into the conditional symbol error probability expressions in the following analysis. The result of the integration is presented in the Appendix.

The conditional symbol error probability for the direct branch, $P\left(e|\left\{\mathfrak{D},\gamma_{\mathfrak{D}} > \gamma_T\right\}\right)$, follows the symbol error probability for a direct link between two nodes using SSD with the link SNR greater than γ_T. This can be expressed using the $I_{SSD}\left(\cdot\right)$ function as:

$$P\left(e|\left\{\mathfrak{D},\gamma_{\mathfrak{D}} > \gamma_T\right\}\right) \geq \int_{\gamma_T}^\infty P^{SD}\left(e|\gamma_{SD}\right)f_{\gamma_{SD}}\left(\gamma\right)d\gamma \geq I_{SSD}\left(a,b,\overline{\gamma}_{SD},\gamma_T,\theta\right) \tag{B.28}$$

where the average SNR $\overline{\gamma}_{SD}$ is the average SNR of the link itself and not the average decision SNR, and $P^{SD}(e|\gamma_{SD})$ represents the symbol error probability of the $S-D$ link conditioned upon the SNR. This is not an exact representation of the symbol error probability for the $S-D$ link, but an approximation. The effect of the approximation will be shown in the results section.

The symbol error probability for the relayed branch can be derived by considering the symbol error probability for a two-hop relayed link. Expressed using the inverse of correct reception across both hops, we get:

$$\begin{aligned} P\left(e|\left\{\mathfrak{R}, \gamma_{\mathfrak{R}} > \gamma_T\right\}\right) &\geq 1 - \left[1 - P^{SR}(e)\right]\left[1 - P^{RD}(e)\right] \\ &\geq P^{SR}(e) + P^{RD}(e) - P^{SR}(e)\, P^{RD}(e) \end{aligned} \tag{B.29}$$

where $P^{SR}(e)$ and $P^{RD}(e)$ independently represent the symbol error probability in the $S-R$ and $R-D$ channels respectively. Similar to the $S-D$ link, the symbol error probability in the $R-D$ link follows the symbol error probability of a direct link employing SSD with the link SNR greater than γ_T:

$$P^{RD}(e) \geq \int_{\gamma_T}^{\infty} P^{RD}(e|\gamma_{RD})\, f_{\gamma_{RD}}(\gamma)\, d\gamma \geq I_{SSD}(a, b, \overline{\gamma}_{RD}, \gamma_T, \theta) \tag{B.30}$$

The symbol error probability for the $S-R$ channel, however, needs to take into account the PRS protocol. Using the PDF from (B.12) with expectation given by the average link SNR results in the following expression for the symbol error probability:

$$\begin{aligned} P^{SR}(e) &\geq \int_{\gamma_T}^{\infty} P^{SR}(e|\gamma_{SR})\, f_{\gamma_{SR}}(\gamma)\, d\gamma \\ &\geq \int_{\gamma_T}^{\infty} P^{SR}(e|\gamma_{SR}) \sum_{i=1}^{N} \binom{N}{i} (-1)^{i-1} \left[\frac{i}{\overline{\gamma}_{SR}} \exp\left(\frac{-i\gamma}{\overline{\gamma}_{SR}}\right)\right] d\gamma \\ &\geq \sum_{i=1}^{N} \binom{N}{i} (-1)^{i-1} I_{SSD}(a, b, \overline{\gamma}_{SR}/i, \gamma_T, \theta) \end{aligned} \tag{B.31}$$

Substituting (B.30) and (B.31) into (B.29) gives the symbol error probability for the relayed branch. Note that setting $z = 0$ gives the symbol error probability for the expressions not conditioned upon the SNR being greater than the threshold, i.e. $P(e|\mathfrak{R})$ and $P(e|\mathfrak{D})$. Finally, substituting (B.29) and (B.28) into (B.21) along with the respective selection probabilities gives the final probability of error for the DSSC-PRS-SSD system.

Due to clustering, all relays are assumed to share the same average channel SNR both from the source and to the destination [11]. The average inter-nodal SNRs have remained independent in the analysis, facilitating analysis of the system with a stronger relayed link relative to the direct link, a favourable condition for employing relaying which will be considered in Section 4.

3.2 Spectral Efficiency

Cooperative communication systems suffer from poor spectral efficiency relative to other spatial diversity systems. DSSC systems, however, have been shown to provide better spectral efficiency than other cooperative systems such as DSC [11] and N relay forwarding systems [4]. It is therefore of interest to compute the spectral efficiency of the DSSC-PRS-SSD system since, as discussed in Section 2, the spectral efficiency of the DSSC-PRS system is affected by the addition of SSD due to changes made to the system model.

The spectral efficiency of the DSSC-PRS-SSD system can be computed by considering the steady state branch selection probabilities and the probability of branch switching. This gives the following expression for the average spectral efficiency:

$$\tilde{q} = p_{\mathfrak{D}} \left[\left(1 - F_{\gamma_{\mathfrak{D}}}\left(\gamma_T\right)\right) q + F_{\gamma_{\mathfrak{D}}}\left(\gamma_T\right) \frac{q}{2} \right] + p_{\mathfrak{R}} \left[\left(1 - F_{\gamma_{\mathfrak{R}}}\left(\gamma_T\right)\right) \frac{q}{2} + F_{\gamma_{\mathfrak{R}}}\left(\gamma_T\right) \frac{2q}{3} \right] \quad \text{(B.32)}$$

where q is the spectral efficiency of non-cooperative direct transmission, $\tilde{q}$ is the average spectral efficiency of the DSSC-PRS-SSD system, and $F_{\gamma_{\mathfrak{D}}}\left(\gamma_T\right)$ and $F_{\gamma_{\mathfrak{R}}}\left(\gamma_T\right)$ are defined in (B.19) and (B.17) respectively.

4. Numerical Results and Simulations

In this section we present numerical results validated with simulations for the DSSC-PRS-SSD system, investigating error performance, spectral efficiency and the effect of variations in channel strengths. The optimum switching threshold is used in all cases, obtained from minimization of the relative performance bound. The optimum rotation angle of $31.7°$ [20] is used throughout with 4-QAM modulation. It was found through simulation that the optimum rotation angle for the DSSC-PRS-SSD system is unchanged from that of a direct transmission SSD system. Simulations are performed over quasi-static flat fading Rayleigh channels with AWGN as described in section 2, with a block length of 100. It is assumed that full CSI is available at all receiving nodes.

Figure B.3 shows the SER of the DSSC-PRS-SSD system using the MDLB with $N = 1$ and $N = 3$ relays along with simulation results for comparison. Also shown is the SER of the DSSC-PRS system without SSD.

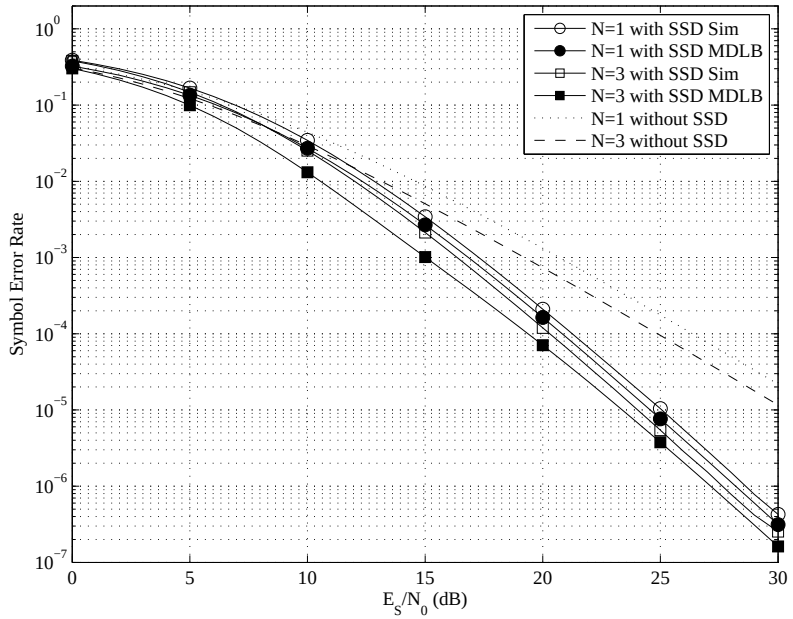

Figure B.3: SER of DSSC-PRS with and without SSD for $N = 1$ and $N = 3$ relays

The lower bound on the SER is within 0.3dB of simulation results at the chosen rotation angle for a single relay, and within 0.5dB for $N = 3$ relays in the asymptotic high SNR region, validating the performance analysis. The error induced by the approximation to the SER for each link appears to increase with an increase in N. Clearly, the addition of SSD

to the DSSC-PRS system has brought about substantial SER performance and diversity gains. At an error rate of 10^{-4}, the DSSC-PRS-SSD system outperforms the DSSC-PRS system by approximately 5dB. The SER improvement will continue to grow as the SER decreases due to the diversity increase, thus partially alleviating the relatively poor error performance of the DSSC-PRS system. However, similar to the non-SSD case, it is readily apparent from the figure that no diversity order increase is attained with an increase in the number of cooperating relays. The SER merely improves by approximately 1dB when N is increased from 1 to 3.

Figure B.4 shows simulation results for the SER of DSSC-PRS-SSD for $N = 1$, $N = 3$ and $N = 5$ relays. It is clear that for the system with SSD, increasing the number of relays beyond 3 does not result in any further SER performance or diversity gains, similar to the system without SSD [11].

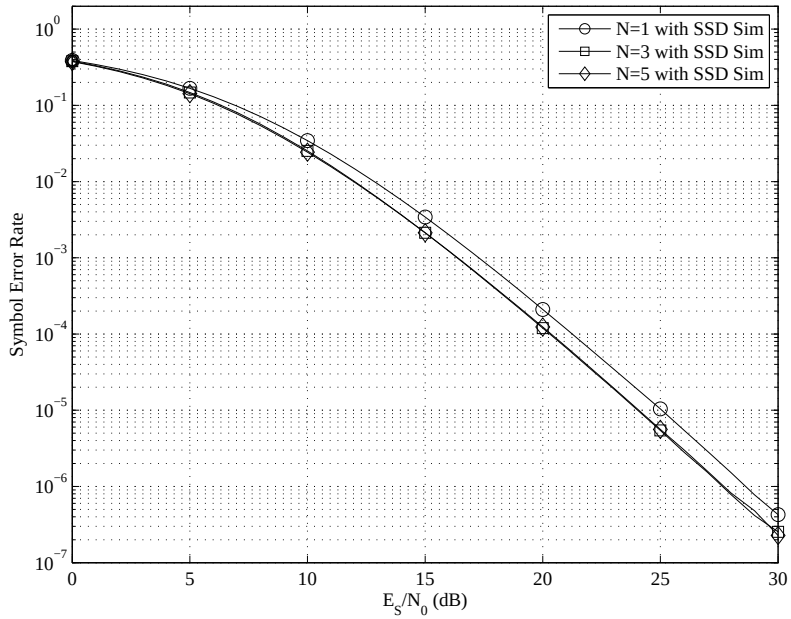

Figure B.4: SER simulation of DSSC-PRS-SSD with differing values of N

A potentially stronger relay link is one of the primary motivators for the use of cooperative communication. Hence, we investigate the effect of a stronger relay path on the DSSC-PRS-SSD system. Figure B.5 plots the SER for the single relay case with varying channel strengths using the derived MDLB. The change in channel strength is indicated by a multiplicative factor λ for any given channel, i.e. the new strength is given by $\lambda\overline{\gamma}$.

It is clear that the best SER performance is attained with a strong $S-D$ channel when $\lambda = 10$; however this is an unfavourable condition for cooperation and should be avoided. With a strong

$S - R$ channel (or a strong $R - D$ channel which produces the same result), the SER decrease is marginal as the probability of error in the $R - D$ channel is unchanged, as expected. With strong channels both to and from the relay, substantial gain is achieved, equivalent to the gain from a strong $S - D$ channel at high SNR and an improvement of close to 4dB. This is the most favourable condition for relaying. Increasing the channel strength factor to $\lambda = 20$ both to and from the relay results in a further SER improvement of approximately 1dB as expected.

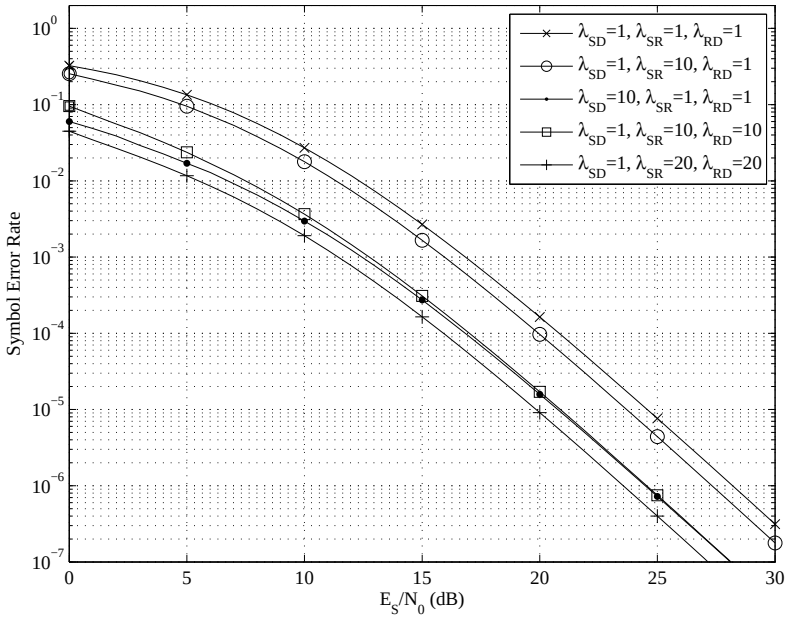

Figure B.5: SER for $N = 1$ relay and various channel strengths

Even though employing more than a single relay does not significantly improve SER performance, it can increase resilience to shadowing and other fading effects, especially if the relays happen to be moving mobile terminals. However, as shown in [11], spectral efficiency decreases with an increase in the number of relays due to the relayed link benefitting from an improved SNR, and hence being utilized more often. However, spectral efficiency is still higher than that of DSC [11].

We compare the spectral efficiency attained by the DSSC-PRS-SSC system to other non-SSD systems using the derived spectral efficiency expression from Section 3.2. Figure B.6 plots the spectral efficiency against the average SNR for DSSC-PRS with and without SSD, and the boundary cases of direct transmission and DSC [11] (note that DSC represents higher spectral efficiency than N relay forwarding systems). Clearly, the addition of SSD has reduced the spectral efficiency at low SNR due to Case 4 occurring more often, however at high SNR the spectral efficiency approaches the non-SSD system. As with the non-SSD system [11],

increasing the number of relays results in decreased spectral efficiency compared to a single relay system.

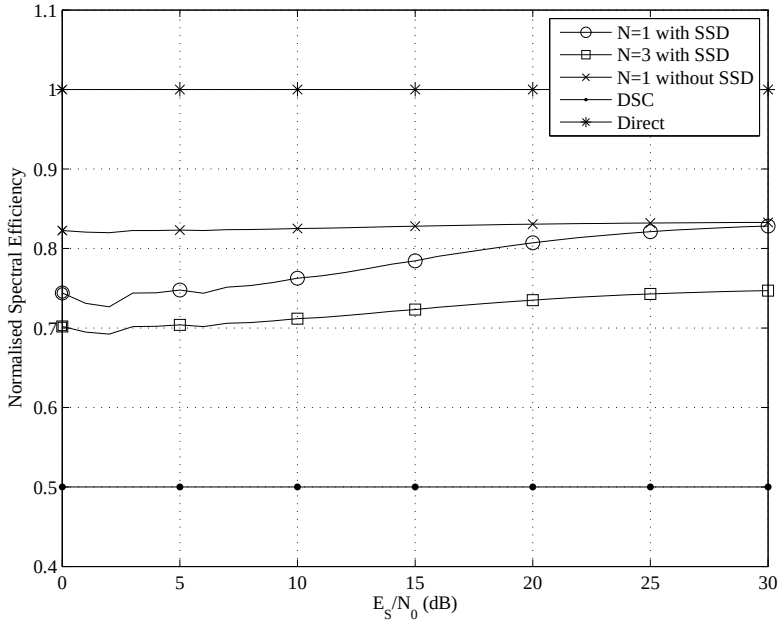

Figure B.6: Spectral efficiency of DSSC-PRS with and without SSD

5. Conclusion

SSD has been successfully incorporated into a DSSC-PRS system to alleviate its comparatively low error performance. Doing so necessitated a change to the system model which consequently decreases spectral efficiency at low SNR. Analytical results were presented in the form of a lower bound on the SER and were found to closely approximate the simulation results. The DSSC-PRS-SSD system was found to outperform the conventional DSSC-PRS system by approximately 5dB at an SER of 10^{-4}, making the addition of SSD a better proposal for increasing error performance and diversity when compared to schemes such as DSC which suffer from lower spectral efficiency. Overall, the addition of SSD to the system provides substantial SER performance gain, with an increase in detector complexity and slight decrease in spectral efficiency at low SNR as penalty.

6. Appendix

The $I_{SSD}(\cdot)$ function can be expressed as:

$$I_{SSD}(a,b,c,z,\theta) = \int_z^\infty \int_z^\infty \left[\begin{array}{l} 4aQ\left(\sqrt{b\zeta}\right) - \\ 4a^2Q^2\left(\sqrt{b\zeta}\right) \end{array} \right] \left[\begin{array}{l} \frac{1}{c}\exp\left(\frac{-\gamma_1}{c}\right) \times \\ \frac{1}{c}\exp\left(\frac{-\gamma_2}{c}\right) \end{array} \right] d\gamma_1 d\gamma_2$$

$$= \frac{a}{n} \left\{ \begin{array}{l} \frac{1}{2}\left(\frac{2}{bc\cos^2\theta+2}\right)\exp\left(-z\left[\frac{bc\cos^2\theta+2}{2c}\right]\right) \times \\ \left(\frac{2}{bc\sin^2\theta+2}\right)\exp\left(-z\left[\frac{bc\sin^2\theta+2}{2c}\right]\right) \\ -\frac{a}{2}\left(\frac{1}{bc\cos^2\theta+1}\right)\exp\left(-z\left[\frac{bc\cos^2\theta+1}{c}\right]\right) \times \\ \left(\frac{1}{bc\sin^2\theta+1}\right)\exp\left(-z\left[\frac{bc\sin^2\theta+1}{c}\right]\right) \\ +(1-a)\sum_{d=1}^{n-1} \left(\frac{S_d}{bc\cos^2\theta+S_d}\right)\exp\left(-z\left[\frac{bc\cos^2\theta+S_d}{cS_d}\right]\right) \times \\ \quad \left(\frac{S_d}{bc\sin^2\theta+S_d}\right)\exp\left(-z\left[\frac{bc\sin^2\theta+S_d}{cS_d}\right]\right) \\ +\sum_{d=n}^{2n-1} \left(\frac{S_d}{bc\cos^2\theta+S_d}\right)\exp\left(-z\left[\frac{bc\cos^2\theta+S_d}{cS_d}\right]\right) \times \\ \quad \left(\frac{S_d}{bc\sin^2\theta+S_d}\right)\exp\left(-z\left[\frac{bc\sin^2\theta+S_d}{cS_d}\right]\right) \end{array} \right\} \tag{B.33}$$

where $\zeta = \gamma_1\cos^2\theta + \gamma_2\sin^2\theta$, $S_d = 2\sin^2(d\pi/4n)$ and n is the total number of iterations used in the approximation.

7. References

[1] T. Eng, N. Kong, and L. B. Milstein, "Comparison of diversity combining techniques for Rayleigh-fading channels," *IEEE Trans. Commun.*, vol. 44, no. 9, pp. 1117–1129, Sep. 1996.

[2] J. N. Laneman, D. N. C. Tse, and G. W. Wornell, "Cooperative diversity in wireless networks: Efficient protocols and outage behavior," *IEEE Trans. Inf. Theory*, vol. 50, no. 12, pp. 3062–3080, Dec. 2004.

[3] J. Boutros and E. Viterbo, "Signal space diversity: A power- and bandwidth-efficient diversity technique for the Rayleigh fading channel," *IEEE Trans. Inf. Theory*, vol. 44, no. 4, pp. 1453–1467, Jul. 1998.

[4] J.-W. Kwon, Y.-C. Ko, and H.-C. Yang, "Maximum spectral efficiency of amplify-and-forward cooperative transmission with multiple relays," *IEEE Trans. Wireless Commun.*, vol. 10, no. 1, pp. 49–54, Jan. 2011.

[5] Y. Zhao, R. Adve, and T. J. Lim, "Improving amplify-and-forward relay networks: Optimal power allocation versus selection," *IEEE Trans. Wireless Commun.*, vol. 6, no. 8, pp. 3114–3123, Aug. 2007.

[6] Z. Yi and I. Kim, "Diversity order analysis of the decode-and-forward cooperative networks with relay selection," *IEEE Trans. Wireless Commun.*, vol. 7, no. 5, pp. 1792–1799, May 2008.

[7] H.-C. Yang and M.-S. Alouini, "Performance analysis of multibranch switched diversity systems," *IEEE Trans. Wireless Commun.*, vol. 51, no. 5, pp. 782–794, May 2003.

[8] D. S. Michalopoulos and G. K. Karagiannidis, "Distributed switch and stay combining (DSSC) with a single decode and forward relay," *IEEE Commun. Lett.*, vol. 11, no. 5, pp. 408–410, May 2007.

[9] —, "Two-relay distributed switch and stay combining," *IEEE Trans. Commun.*, vol. 56, no. 11, pp. 1790–1794, Nov. 2008.

[10] I. Krikidis, J. Thompson, S. McLaughlin, and N. Goertz, "Amplify-and-forward with partial relay selection," *IEEE Commun. Lett.*, vol. 12, no. 4, pp. 235–237, Apr. 2008.

[11] V. N. Q. Bao and H. Y. Kong, "Distributed switch and stay combining with partial relay selection over Rayleigh fading channels," *IEICE Trans. Commun.*, vol. 93, no. 10, pp. 2795–2799, Oct. 2010.

[12] S. A. Ahmadzadeh, S. A. Motahari, and A. K. Khandani, “Signal space cooperative communication,” *IEEE Trans. Wireless Commun.*, vol. 9, no. 4, pp. 1266–1271, Apr. 2010.

[13] W. Ning, Z. Zhongpei, and L. Shaoqian, “Signal space diversity in decode-and-forward cooperative communication,” in *Proc. WRI Int. Conf. Communications and Mobile Computing*, 2009, pp. 127–130.

[14] Z. Paruk and H. Xu, “Performance analysis and simplified detection for signal space diversity with MRC reception,” *SAIEE Africa Research Journal*, 2012, submitted for publication.

[15] T. Wang, A. Cano, G. B. Giannakis, and J. N. Laneman, “High-performance cooperative demodulation with decode-and-forward relays,” *IEEE Trans. Commun.*, vol. 55, no. 7, pp. 1427–1438, Jul. 2007.

[16] A. Papoulis and S. U. Pillai, *Probability, Random Variables and Stochastic Processes*, 4th ed. McGraw Hill Higher Education, 2002.

[17] C. Tellambura, A. Annamalai, and V. K. Bhargava, “Unified analysis of switched diversity systems in independent and correlated fading channels,” *IEEE Trans. Commun.*, vol. 49, no. 11, pp. 1955–1965, Nov. 2001.

[18] M. K. Simon and M. S. Alouini, *Digital Communication Over Fading Channels*, 2nd ed. Wiley-IEEE Press, 2005.

[19] H. Xu, “Symbol error probability for generalized selection combining reception of M-QAM,” *SAIEE Africa Research Journal*, vol. 100, no. 3, pp. 68–71, Sep. 2009.

[20] G. Taricco and E. Viterbo, “Performance of component interleaved signal sets for fading channels,” *IEE Electronics Letters*, vol. 32, no. 13, pp. 1170–1172, Apr. 1996.

Part III

Conclusion

1. Conclusion

Cooperative communication systems are able to offer performance improvements through the exploitation of available spatial diversity in wireless networks. They can also enhance coverage and provide natural resilience to shadowing and fading, although they typically have higher complexity and feedback requirements and reduced spectral efficiency when compared to other spatial diversity techniques such as diversity from multiple antennas. The distributed switch and stay combining with partial relay selection scheme manages to reduce the processing, complexity and feedback requirements for a cooperative communication system; however error performance suffers as a result. This study attempted to improve the error performance of the DSSC-PRS system by incorporating signal space diversity. A simpler expression for the error probability of SSD systems was also derived, along with a simplified maximum-likelihood detection scheme. The results are presented in two papers contained in this dissertation.

In Paper A, SER performance of an SSD system with a single transmit antenna and N receive antennas with MRC reception was presented and validated with simulation. Closed form SER expressions were presented using the conventional union bound and the NN approximation for both 4-QAM and 16-QAM modulation. A new lower bound based on the minimum Euclidean distance of a rotated constellation was also presented in closed form. The NN approximation was found to have tighter SER performance than the conventional union bound at high SNR, and the new MDLB, while tight at low SNR, is looser than the union bound/NN approximation at high SNR for single antenna reception. However, SER performance of the new MDLB was found to improve with an increase in the number of receive antennas.

The proposed simplified detection scheme was successfully implemented and, while losing diversity with single antenna reception, attains SER performance within 1dB of optimal detection at an SER of 10^{-3} for 16-QAM with a complexity reduction in terms of the average number of searches required of 61% ($m = 9$). Reducing the complexity further to 75% ($m = 5$) for 16-QAM degrades SER performance with single antenna reception. The simplified detection scheme is able to achieve SER performance close to indistinguishable from optimal detection with multiple antenna reception. This is achieved for $N = 3$ with $m = 9$, giving complexity reductions of 61% and 88% for 16-QAM and 64-QAM respectively; and for $N = 4$ with $m = 5$, resulting in complexity reductions of 75% and 93% respectively.

In Paper B, SSD was incorporated into a DSSC-PRS system to alleviate the error performance penalty introduced by DSSC. SER analysis was performed using the MDLB derived in Paper

A and was found to be in agreement with simulation results. It was found that employing SSD in the DSSC-PRS system brings an SER improvement of approximately 5dB at an error rate of 10^{-4} along with an increase in diversity order.

The spectral efficiency of the new system was also evaluated and found to be reduced at low SNR compared to the system without SSD due to the changes made to the system model, however at high SNR, spectral efficiency approaches that of the system without SSD. The effect of variations in channel conditions was also evaluated with the new system; it was found that the best SER performance was attained when the relay link was strongest, which is also the most favourable condition for relaying.